FROM SKIN TO NEURONS: EXAMINING VARIATIONS IN REPROGRAMMING EFFICIENCY

 $\mathbf{B}\mathbf{y}$

Sarah A Keaton

A THESIS

Submitted to Michigan State University in partial fulfillment of the requirements for the degree of

Physiology- Master of Science

2013

ABSTRACT

FROM SKIN TO NEURONS: EXAMINING VARIATIONS IN REPROGRAMMING EFFICIENCY

By

Sarah A Keaton

Cellular reprogramming is a newly emerging field with promising clinical applications. The ability to generate non-dividing crucial cell types from rapidly proliferating cell types, the potential to heal diseased people who do not have many treatment options, being able to bypass immune rejection, and avoid invasive surgery has captured the media's attention. However, there have been disparities in the efficiency of reprogramming and these needs to be addressed before cellular reprogramming can be applicable in a clinical setting. To better understand the variations of cellular reprogramming, human and mouse fibroblasts were converted into induced neuralcells in an attempt to unveil the impact of disease state, tissue origin and genetics. The experimental results indicatereprogramming efficiency was reproducible within a primary fibroblast line however there was a dramatic difference between lines even from an isogenic source. Testing a larger number of fibroblast lines, even lines with the identical genetic backgrounds and tissue origins, is likely the most direct means of improving reprogramming efficiency and enabling this procedure to be available for therapeutic use

Dedicated to my parents,	Karen and Patrick encouraged me to	Keaton, who have keep questioning.	always supported me and

ACKNOWLEDGEMENTS

I would like to thank my committee members, Dr. Jose Cibelli, Dr. Susanne Mohr, Dr. Steve Suhr, and Dr. Robert Wiseman. I would also like to acknowledge my fellow laboratory members past and present in their support and for the production and maintenance of fibroblast lines used in this thesis. Finally, I would like to thank the Physiology staff and fellow students for always being there to help me advance myself educationally.

TABLE OF CONTENTS

LIST OF TABLES.	vi
LIST OF FIGURES	vii
KEY TO ABBREVIATIONS	X
INTRODUCTION	1
CELLULAR REPROGRAMMING	1
APPLICATION OF CELLULAR REPROGRAMMING	
GENERAL PROBLEMS IN CELLULAR REPROGRAMMING	
GENERAL PURPOSE OF THIS STUDY	3
DIRECT CELLULAR REPROGRAMMING	3
iPSC CONVERSION	
EFFICIENCY DIFFICULTY	5
FIBROBLAST CELLS AS AN INPUT LINE	7
NEURONS AS AN OUTPUT CELL	
CLINICAL APPLICATION AND NEUOLOGIC DISORDERS	8
PURPOSE OF THIS STUDY	11
METHODS	12
FIBROBLAST LINES.	
FIBROBLAST CHARACTERIZATION.	
inc induction.	
IMMUNOHISTOCHEMISTRY AND IMAGING.	
ELECTROPHYSIOLOGY	
HUMAN NPC CULTURE AND NEURON DERIVATION	23
QUANTIFICATION OF INC CONVERSION	31
RESULTS	31
CONCLUSIONS	49
REFERENCES	53

LIST OF TABLES

Table 1: General Properties of Fibroblast Lines. Study ID, abbreviated line designation used this report; Line ID, line common name; Donor, donor health status or strain; Sex, sex of donor (male, female, or of mixed sex); Age, age of donor (years, unless otherwise noted); Tissue, fibroblast tissue of origin. mRNA Expression: results of quantitative PCR analysis of multiple markers. COL1A2, fibroblast marker collagen type I alpha 2; FNECTIN, fibroblast marker fibronectin; FIBR1, fibroblast marker fibrillin I; FIBU5, fibroblast marker fibulin V; VIM, fibroblast marker vimentin; KER14, keratinocyte marker keratin 14; PECAM, endothelial cell marker Platelet endothelial cell adhesion molecule/CD31; FOXG1, neural progenitor marker Forkhead box protein G1; SOX2, neural progenitor marker SRY (sex determining region Y)- box 2, MYOD, myogenic progenitor marker MyoD1; MYF5, myogenic progenitor marker myogenic factor 5. Immunocytochemistry: summary of immunocytochemical analysis of fibroblastassociated (fibronectin, vimentin) and stem cell-associated markers (Sox-2, nestin) in fibroblast lines. N/A, not applicable; ND, –not done; +, positive; –, weakly positive; -, negative. (From Table 2: Primers Used in Cloning and qRT-PCR Analysis. Cloning- primers used in the amplification of cDNAs or plasmid DNA for construction of retroviral vectors; QPCR- primers used in qRT-PCR quantification of gene expression. The species of the gene targeted by each

LIST OF FIGURES

Figure 1:Time Course of induced Neural Cell (iNC) Induction and Electrophysiological Analysis. (A) Examples of untransduced fibroblasts or fibroblasts infected with a YFP-only control vector (green) cultured under INC induction conditions for 4 weeks and stained for TUJ1 (red). (B) TUJ1-, SYN1-, and MAP2-positive mouse and human iNCs over time expressed as a percentage of the maximum TUJ1 value. Infection was at time 0 (T0), T1 = 8–10 days, T2 = 18– 20 days, and T3 = 28–30 days. (C) Examples of human iNCs produced by different fibroblast lines at the T1-T3 time points (labeled on left) and stained for TUJ1 (red). In the upper left panel, arrows indicate early iNCs in a low-magnification field. In the upper right panel, the iNC boxed at the left is shown magnified for each color channel and the merged image. In the center and lower panels, iNCs at the T2 and T3 time points, respectively, are shown. Scale bars are 10 mm unless otherwise noted. Insets depict the cell soma with the blue channel removed to more clearly reveal iNC factor expression. (D) Representative electrophysiological recordings from iNCs. Upper left panel - Isolated voltage-gated sodium current recorded from a representative human iNC. Upper records show voltage steps from a holding potential of - 80mV to test potentials of -40, -25, 0, and 25 mV. Lower records show leak-subtracted Na + current elicited by these voltage steps. Note that the step to - 40mV is sub threshold and that the steps to - 25, 0 and 25mV are supra-threshold and elicit inward sodium current of amplitude and kinetics which is voltage dependent. Inset shows the relationship of test potential and the maximum amplitude of the Na + current elicited at each test potential in this cell. Upper right panel—Voltage-gated inward Na+ current was blocked by TTX. Upper record: voltage step from - 80 to 0 mV, which was repeated every 2.5 s during the recording. Lower records: current elicited by the membrane depolarization at different times during the recording. Voltage-gated inward Na+ current (but not outward K+ current) was reduced in a time-dependent manner after the application of TTX (5 mM) to the extracellular medium. Lower panels—Representative action potentials (APs) recorded from NPC-neurons and INCs. Left - AP produced by an NPC-derived neuron. Membrane potential change (upper record) elicited by application of membrane current step (lower trace) while holding the membrane at - 72mV just before current step application. Center—AP produced by an ADF iNC. Membrane potential changes (upper records, x and y) elicited by application of membrane current step (lower trace) without (x) and with (y) holding the membrane at - 90mV (x) or - 55mV (y) just before current step application. Right—Overlay of the NPC and INC AP traces (NPC, green; ADF, red)Top Panel: Raw tracings for visual reference only.(From Alicea et al. 2013 [54])For interpretation of the references to color in this and all other figures, the reader is referred to the electronic version of this thesis......24

Figure 2:Immunocytochemical Analysis of Human and Mouse Fibroblast Lines. (A) Immunostaining of human cell lines with anti-vimentin (red) and anti-nestin (green) antibody. Upper panels—both antibodies in all fibroblast cell lines as labeled. Middle panels—the green channel only (nestin), displaying an absence of positive signal. Lower panels controls showing the same antibodies on human NPCs as labeled. (B) As in A, with anti-fibronectin (red) and anti-Sox2 (green) antibodies. Insets in middle panels show magnified images, indicating that rare spots of faint green fluorescence are not cell/ nucleus associated as with genuine Sox-2 immunopositivity observed in NPCs. (C, D) As in A and B for selected mouse fibroblast lines.

The panels at the end show that as with human cells, rare patches of faint green fluorescence do not co-localize with nuclei and do not indicate Sox-2 immunoreactivity. Blue color in all images is nuclear DNA stain bis-benzimide.(From Alicea et al. 2013 [54])For interpretation of the references to color in this and all other figures, the reader is referred to the electronic version of this thesis
Figure 3:Morphology and Derivation of Fibroblast Lines Used in Analysis. (A) Morphology of the seven human fibroblast lines used for analysis. (B) Outgrowth of fibroblasts and other cell types from tissue fragments of eight mouse tissues at 1 week post plating. The dark mass in the upper left corner is the adherent tissue fragment itself. (C) Morphology of the twelve mouse fibroblast lines (at passage 6) used for analysis
Figure 4:Fibroblast- and Nonfibroblast-associated mRNA Expression in Human and Mouse Fibroblast Lines. Heat map color is proportional to expression level—bright green is high expression and black is no detectable transcript.COL1A2, collagen type 1a2; FNECTIN, fibronectin; FIBR1, fibrillin I; FIBU5, fibulin V; KER14, keratin 14. (From Alicea et al. 2013 [54])For interpretation of the references to color in this and all other figures, the reader is referred to the electronic version of this thesis
Figure 5:Schematic of the NITSC MMLV Retrovirus and YFP Fusion Factors. LTR, long terminal repeat; Ψ+, stem-cell permissive packaging sequence; NEO, G418-resistance gene; I, IRES element; TTA, tet-transactivator; To, tetoperator. (From Alicea et al. 2013 [54])

Figure 6:Induced Neural Cell (iNC) Conversion of Mouse and Human Fibroblast Lines. (A) HEK cells transfected with YFP fusion protein for iNC conversion, as labeled. Phase-contrast images are in the upper panels, and corresponding fluorescent images are in the lower panels. (B) Mouse embryonic fibroblasts infected with the individual factors (as labeled) and stained for β-III-tubulin/TUJ1 in red (upper panels). Mouse (MEFs) or human fibroblasts (FET) infected with combinations of Zic1/ Asc11/Pou3f2 (ZAP) or Myt1L/Asc11/Pou3f2 (MAP) + NeuroD1 (MAPN) (lower panels). Green fluorescence indicates expression of reprogramming factor(s). Blue color is bis-benzimide nuclear staining of DNA. Insets have the blue channel removed and the green channel intensified to show YFP-factor expression in the nucleus of all iNCs. (C) Mouse iNCs produced from MEFs by day 10–15 post-infection immune positive for multiple neural markers (red), including MAP2, pan-neurofilament (NF), doublecortin (DCX), or synapsin I (SYN), iNCs produced from adult mouse fibroblast lines (as labeled) with typical iNC morphology immunostained for β-III-tubulin/TUJ1(red). (D) Human iNCs with typical morphology at day 24–30 post-infection and immunostained for multiple neuronal markers as in (C) in addition to PSD95, GABA receptor b 3 (GABARB3), and GAD1 (as labeled). GABAR-B3 and GAD1 iNCs were labeled using immunoperoxidase secondary antibody coupled with DAB staining. Scale bars are 10 mm unless otherwise labeled. (E) Relative conversion of mouse fibroblast lines to iNCs calculated as a function of cell number at the time of harvest. The highest efficiency of conversion within each group was set to a value of 100. Bars indicate standard error of the mean (SEM). (F) As in E, for the human fibroblast lines. (From Alicea et al. 2013 [54])For interpretation of the references to color in this and all other figures, the reader is referred to the

electronic version of this thesisTop Legend (Left to Right): VIMENTIN NESTIN DNA. DATA (Left to Right): FET, NWB, RET, AUT, SAF, ADF, EAF, E2F. Middle Legend: NESTIN. DATA (Left to Right): FET, NWB, RET, AUT, SAF, ADF, EAF, E2F. Bottom Legend: HUMAN NPCS. DATA (Left to Right): VIMENTIN DNA, VIMENTIN, NESTIN DNA, NESTIN. B) Top Legend (Left to Right): FIBRONECTIN SOX2 DNA. (Left to Right): FET, NWB, RET, AUT, SAF, ADF, EAF, E2F. Middle Legend: Sox2. DATA (Left to Right): FET, NWB, RET, AUT, SAF, ADF, EAF, E2F. Bottom Data (Left to Right): FIBRONECTIN DNA, FIBRONECTIN, SOX2 DNA, SOX2. C) Top Legend (Left to Right): VIMENTIN NESTIN DNA. Data (Left to Right): HE4, KI3, KI5, KI6, LI6, SM1, TA4, TE4, TE5. Middle Legend: Nestin. Data (Left to Right): HE4, KI3, KI5, KI6, LI6, SM1, TA4, TE4, TE5. Bottom Legend: Data (Left to Right): HE4, KI3, KI5, KI6, LI6, SM1, TA4, TE4, TE5.D) Top Legend: (Left to Right): FIBRONECTIN SOX2 DNA. Data (Left to Right): HE4, KI3, KI5, KI6, LI6, SM1, TA4, TE4, TE5. Bottom Legend: SOX2 Data (Left to Right): HE4, KI3, KI5, KI6, LI6, SM1, TA4, TE4, TE5. Bottom Legend: SOX2 Data (Left to Right): HE4, KI3, KI5, KI6, LI6, SM1, TA4, TE4, TE5. Bottom Legend: SOX2 Data (Left to Right): HE4, KI3, KI5, KI6, LI6, SM1, TA4, TE4, TE5.

KEY TO ABBREVIATIONS

DNA Deoxyribonucleic acid

DS Donkey serum

HEK Human Embryonic Kidney 293

iNC Induced neuron cell

iPSC Induced pluripotent stem cell

MECP2 Methyl-CpG-binding protein 2

MEFs Mouse embryonic fibroblast

MMLV Moloney murine leukemia virus

MOI Multiplicity of infection

NPCs Neural Progenitor Cells

ORFs Open reading frames

PBST PBS with 0.3% Triton X-100

PORN/lam Polyornithine/laminin

PCR polymerase chain reaction

qPCR Quantitative polymerase chain reaction

RT-PCR Quantitative real-time polymerase chain reaction

Vcon Conditioning potential

Vh Holding potential

Vtest Testing potential

VSV Vesicular stomatitis virus

YFP Yellow fluorescent protein

ZAP YZIC/YASCL/YPOU3F

INTRODUCTION

CELLULAR REPROGRAMMING

Cellular reprogramming is an important and relatively new field in medicine that has the potential to heal diseased people whoface minimal treatment options. Cellular reprogramming describes the process by which a fully differentiated, somatic (non-germ line) cell type is induced to convert to a different cell type. If not for cellular reprogramming, this conversion would not be observed under normal physiological conditions [1]. With the possibility of converting an abundant, readily available cell type into a scarce, crucial cell type required to maintain physiological homeostasis, the new and potentially auspicious field of cellular reprogramming is deserving of research attention.

APPLICATION OF CELLULAR REPROGRAMMING

The concept of generating new, non-proliferating cell types from a patient's own cells coupled with the ability to bypass the chance of immune rejection is a promising aspect of cellular reprogramming research. Furthermore, this technique aids in the replenishment of crucial and scarce host cells under a dissimilar, currently-existing genetic program. As a result, application of potentially toxic and harmful pharmaceuticals may be bypassed.

Spinal cord injury serves as an example of the ways in which direct cellular reprogramming could have therapeutic benefits for those with little hope due to the current absence of curative therapy. Currently, care in the acute and sub-acute to chronic phases are severely limited to high-dose corticosteroid treatment intended to reduce inflammation, surgical stabilization and decompression to reduce further damage with focus placed on symptomatic relief [2]. Spinal cord injury severs axons causing the distal segment of the axon to degenerate, disrupting motor control and sensory input below the level of the lesion [3].

A taylored of the cellular reprogramming regimen could permit rehabilitation of a patient who has suffered a severe injury resulting in paraplegia with the use of their own cells. Hypothetically, a skin biopsy could be obtained from the patient for isolation of the fibroblasts followed by reprogramming to induced neural cells (iNCs) via transcription factors *in vitro*. The iNCs could be injected back into the patient at the site of injury. With proper establishment and incorporation into the nervous system network, this process could aid in healing the patient. Currently this practice is not clinically available. However with increased efficiency and research in reprogramming techniques, this may be a viable option with clinical applications in the future.

The future clinical application of cellular reprogramming may revolutionize the ways in which acute injures are currently treated. Immunosuppressive drugs will likely be mandatory with rapid administration to evade immune flare-up. It may be possible or necessary to preprime these cells through exposure to stressful environments and cell repositories may be available in case of injury.

The present study examines the process of direct cellular reprogramming and the components that influence the efficiency of converting human and mouse fibroblasts into functional iNCs. Research such as this may very well be a step toward future clinical applications of cellular respecification with unprecedented medicinal benefit.

GENERAL PROBLEMS IN CELLULAR REPROGRAMMING

As stated previously, cellular respecification is not an available means of clinically treating ailments at this time for various reasons. A primary issue with the process is conversion efficiency. When exploring multiple reprogramming regimens -irrespective of the input or desired output cell type- the efficiency of conversion is subpar. This issue must be addressed in order to move toward clinical applications.

Without increased efficiency, the quantity of input cell type required for harvest would be far too large to allow the diseased patient to return to physiological homeostasis. Without the knowledge and proper understanding of this phenomenon, application of this respecification regimen on human subjects cannot be justified due to the risk of detrimental effects. What is priming certain cells to be capable of conversion to a different cell type, while others are unable to reprogram at all? In addition, if the cells are capable, why is the conversion at such low efficiency?

GENERAL PURPOSE OF THIS STUDY

The current study attempts to address the issue of conversion efficiency. If the causes of variable results and generally low observed efficiency rates can be identified, clinical availability of reprogramming regimens might be attainable. Variation exists each time a protocol is performed, whether it is an extra second in the incubator, genetics or specimen origin. In the current study, components of the cell lines will be examined closely including: disease states, genetics and tissue origin to better address what is influencing the variable conversion results.

DIRECT CELLULAR REPROGRAMMING

Direct cellular reprogramming is the process by which a fully differentiated, somatic cell type is induced to convert to a different cell type without reverting to a stem cell-like state. This induced cellular conversion would not occur under normal physiological conditions directly. This specialized area involves the application of transcription factors and/or small molecules to the input cell to induce phenotypic changes.

The majority of cells in an organism differ both, morphologically and functionally from one another in varying degrees. However all cells originate from a single cell, the zygote, and

through multiple cell divisions, the zygote gives rise to all cell types present in a given organism. Most cells in an organism contain exactly the same deoxyribonucleic acid (DNA) sequence, and epigenetics are impacting the gene expression among different cell types [4]. Epigenetics describes "the interactions between genes and the cellular environment that produces a change in the cell phenotype" [5].

In a eukaryotic cell, the DNA is condensed into chromatin within the nucleus.

Transcription factors are proteins that are involved in gene transcription regulation. A transcription factor can interact with DNA nonspecifically to find its binding site where the transcription factor alters conformation and induces transcription by interacting with other proteins. The process of transcription requires transcription factors to bind to regulatory elements of the DNA located near the target genes. Once the transcription factor binds, transcription of the target gene starts [6]. This process can lead to changes in cellular morphology and function. By utilizing the knowledge of transcription factors, it is possible to apply certain transcription factors to reprogram a somatic cell into a different pathway that it would not normally express in physiological homeostasis (i.e. remaining a fibroblast cell).

One of the earliest studies on direct cellular reprogramming achieved success by transfecting the transcription factor MyoD to convert mouse fibroblasts into skeletal muscle myotubes [7]. This study became the first documented demonstration of a single transcription factor acting as a master switch for changing the cell's identity by activating the whole genetic program of muscle differentiation in a non-muscle cell type. Since this first discovery, laboratories have been able to generate functional cardiomyocytes [8], iNCs[9] and induced pluripotent stem cells (iPSCs)[10] from fibroblast cells.

iPSC CONVERSION

Yamanaka was awarded the Nobel Prize for Physiology or Medicine in 2012 for reprogramming human fibroblasts into induced pluripotent stem cells (iPSCs). An increased understanding of the mechanisms by which cellular conversion functions, and the possibilities for the future via his research were gained [10]. One issue with reprogramming into a stem cell is related with the observed genetic instability. A transcription factor used (cMyc) has been reported to promote carcinogenesis [11], and once the cell is converted into a pluripotent state it needs to be converted back to the desired cell type using a variety of reagents that are not present in normal physiology [12]. Therefore, although the generation of iPSCsfrom a fully differentiated cell type is promising and can generate a self-renewing cell type, it has its downfalls.

EFFICIENCY DIFICULTY

With direct cellular reprogramming, the cell is converted from one input cell directly into the desired output cell, consequently saving time and possible error during conversion to a stem cell-like state. An overarching issue for both reprogramming into an iPSC and direct cellular reprogramming is a low conversion rate. There are two subcategories within this issue: the low conversion rate in general, making clinical application less attainable and controversy between different laboratories reporting different results.

Multiple laboratories have reported success with reprogramming cells into different cell types, all demonstrating low efficiency of conversion. Although successful conversion has been demonstrated through both phenotypic and functional data, the amount of the input cells

successfully converted is very low, with only a few input cells converting into output cells while the rest remain in a fibroblastic phenotype [13-16].

Current publications report various conversion rates with the same input cells, and from the same type of input animals to the same type of output cell, causing discrepancy and controversy between differing publications and data. Cell type, species of origin, and age of the donor subject are known variables that could influence reprogramming efficiency. However, even when these properties and technical aspects of the reprogramming regimen are held constant, variation has been observed using direct methods such as infection with recombinant retroviruses or plasmid transduction expressing transcription factors [13-16]. Even one of the first direct cellular reprogramming successes noted reprogramming was not uniform among all cell lines [7]. A comparison of five mouse fibroblast cell lines, C3H10T1/2, NIH3T3, Swiss 3T3, Swiss 3T3 clone 2, and L Cells, transfected with a MyoD expression plasmid and selected to produce colonies of stably transduced cells, yielded colonies of both the input and the conversion phenotype. The conversion efficiency varied dramatically from a maximum of 53% myoblastic colonies in C3H10T1/2 cells to a minimum of 3% myoblastic colonies in L cells all harvested from the same species. Likewise, a published report from Lattanzi et al. [18] that compared the conversion of fibroblasts to myogenic cells from different tissue sources infected with a high titer multiplicity of infection (MOI 2,000) MyoD adenovirus vector found that murine dermis-, muscle-, and bone marrow-derived fibroblasts converted at efficiencies of 59%, 43%, and 7%, respectively, and human fibroblasts derived from the same tissues at efficiencies of 54%, 36%, and 6% respectively.

Together, these reports indicate that conversion variation may be observed irrespective of whether vector delivery is relatively highly efficient (adenoviral infection) or inefficient (plasmid

transduction). More recently, dissimilarity in the input cell population was proposed to account for the conversion disparity of fibroblasts to functional cardiomyocytes as reported by several groups [16, 19-21]. The reason why there is great variation between the results obtained from different groups using the same cell line to convert into a different phenotype is poorly understood.

FIBROBLAST CELLS AS AN INPUT LINE

Fibroblast cells are an ideal cell type for cellular reprogramming due to their high abundance throughout the human body. Fibroblasts are the basic structural unit present in all organs including the skin, and they are involved in the wound healing process. The skin is a superb location clinically to harvest cells because it is easily accessible, therefore less invasive than many surgical procedures. There is also less clinical risk involved in both the healing and harvesting aspects. Fibroblasts are also ideal for use as an input cell because they are easily cultured and are adherent to the plate during experimentation.

Fibroblasts have markers that can be used to confirm their fibroblastic identity which includes vimentin and fibronectin. Vimentin is an intermediate filament protein and is expressed by normal fibroblasts. Vimentin is known to preserve cellular integrity and provide resistance against stress [22]. Fibronectin is another protein, known to play roles in cell adhesion, growth, migration, differentiation and wound healing in adults when expressed [23]. Through examination of these markers, a cell type, which is fibroblastic in nature, may be identified.

NEURONS AS AN OUTPUT CELL

Neurons are specialized cells that are primed for sending and receiving signals, a function that is directly related to structure. The uniquely shaped neuron contains four domains: the cell

body (soma), dendrites, axon, and presynaptic terminals. The cell body surrounds the nucleus, and has been reported to perform many of the neuronal housekeeping functions including synthesis and processing of proteins. The cell body also receives information from outside stimuli. Dendrites are also responsible for receiving information from outside stimuli. The dendrite membranes are covered with receptors that bind and respond to the neurotransmitters released by neighboring cells. The chemical messages of these neighboring cells are translated by membrane receptors into an electrical event that impacts the excitability of the receiving neuron. The cytoplasm of the dendrites contains a dense system of microtubules, making the dendrites plastic and easily remodeled. The axon is similar to the dendrites, but is responsible for the input and output of action potentials to and from the cell body [6].

The axon is longer than dendrites, and the cytoplasm is dense in parallel arrays of microtubules and microfilaments, providing structural stability and rapid movement of materials back and forth between the cell body and the axon terminus. Axons are the message-carrying portion of the neuron, and they are known to carry action potentials to specific target zones. These electrical events (action potentials) can be recorded in a laboratory via patch clamp analysis. The presynaptic terminals are located at the target zone where the axon terminates in multiple endings. These terminals are designed for rapid conversion of the neurons' electrical signal into a chemical signal for the target zones cell to process and act upon [6]. There are multiple types of neurons; however the present study examines iNCs, which can be thought of as an unspecialized neuron-like cell. Neurons are an ideal output cell because they have a reportable and drastic phenotypic change from fibroblasts like the formation of somas, and their change can be reported via functional data of patch clamp analysis.

CLINICAL APPLICATION AND NEUROLOGIC DISORDERS

In the present study, direct reprogramming of fibroblasts from multiple origins into iNCs is explored. This process is clinically relevant due to the prevalence of diseases involving neurons including: Alzheimers, Parkinson's and Hunington's disease. These neurological disorders are characterized by the loss of neurons or neuron functionality, and injections of iNCs at the site of depletion may benefit patients with such neurological disorders. iNCs injections may also be clinically useful at the site of injury for paraplegic patients to reestablish a normal neural network and heal as addressed above.

This study uses two fibroblast lines from people with neurologic disorders. This should provide some insight, but not conclusive evidence, to the capacity of fibroblasts from neurologic disorder patients to iNCs. The two cell lines used came from one patient will Rett Syndrome and another patient with Schizophrenia.

Rett Syndrome is a severe neurodevelopmental disorder affecting primarily females with a ratio of 1:10000 female births. Rett Syndrome is one relatively common genetic cause for severe mental retardation in females. Normal development is observed until 6-18 months of age at which time fine and gross motor skills and social interaction is lost [24]. Most patients also exhibit breathing problems [25] and depending on the case, patients may exhibit seizures and speech problems. Patients undergo devastating motor deterioration, generalized rigidity, dystonia, and worsening of scoliosis. Most patients with Rett Syndrome lose mobility, and are often wheelchair-bound during their teenage years. As patients grow older, they often develop characteristics of Parkinson's disease [26,27].

With this neurodevelopmental disorder, there is an overall decrease in brain and individual neuron size. Autopsy studies have demonstrated a 12%–34% reduction in brain

weight and volume in patients suffering from Rett Syndrome [28]. The Rett Syndrome brain shows no obvious degeneration, atrophy, or inflammation, and there are no signs of neuronal migration defects [29,30]. These observations strongly suggest that Rett Syndrome is a disorder of postnatal neurodevelopment, rather than a neurodegenerative process.

Mutations of the X-linked gene methyl-CpG-binding protein 2 (MECP2) are involved in most Rett Syndrome patients. However precise functional consequences resulting from the mutation of MECP2 and the protein interactions surrounding this mutation remains unknown. The array of mutations includes missense, nonsense, frame shift, and deletions encompassing whole exons. Eight missense and nonsense mutations account for 70% of all mutations [25]. The actual mutation of the patient used in this study is unknown. However, the inclusion of a female patients' fibroblast cell line may provide insight on the potential for a patient with a genetic disorder to produce a cell type that is not functioning properly within their own body.

Fibroblasts harvested from a patient with Schizophrenia are also included in this study. Schizophrenia is a disabling and chronic brain disorder that is still poorly understood, despite its prevalence in society [31]. People with Schizophrenia may exhibit hallucinations, delusions, an increased tendency to perform violent acts, and disordered thinking and behavior. The onset of Schizophrenia is usually post birth. In men, the onset occurs during the teen years into the twenties, while the onset in women occurs somewhat later, typically between twenty and thirty years of age. The cause of onset time is unknown, however it's hypothesized that a multitude of causes are involved, including environment and genetics [32]. Neuroimaging can demonstrate changes within a Schizophrenia patient's brain in comparison with a non-disease type. The loss of cortical gray matter in the brain with evidence of progression over time is one such example of a demonstrable change [33].

PURPOSE OF THIS STUDY

The primary purpose of the present study is to investigate the possible differences in cellular reprogramming capacity between disease subtypes, genetic backgrounds, and tissue origin. One set of cell lines analyzed in this study are primary mouse fibroblasts from various organs. These fibroblasts were all derived from the same mouse, resulting in an identical genetic background among the harvested cells. Through examination of these cell lines, it is possible to discern whether or not genetics plays a role in the ability to reprogram. By removing genetic variation from the equation, it is possible to investigate differences in reprogrammability based solely on the origin of input tissue. In the present study, human fibroblast lines from multiple patients are examined to allow for comparison of the same genetic background to a diverse array.

Through examination of two cell lines, derived from patients with neurologic disorders, it is possible to compare the reprogrammability of a person with a neurodegenerative disorder to that of a healthy individual. The overall goal is to not generate concise conclusions from the data gathered, due to a lack of diseased cell lines applied to the study. However, through such examination, some light may be shed on capacity for reprogrammability. This could be further researched in a future study.

With this knowledge at hand, a better understanding regarding the importance of harvest locations of input cells may be obtained. It is possible that certain harvest locations are primed to exhibit superior efficiency of conversion while other locations are not. Furthermore, multiple questions can begin to be addressed including those regarding the capacity of fibroblasts harvested from a patient with a neurologic disorder to convert to iNCs as well as those regarding variation in genetic background as it relates to conversion efficiency.

METHODS

FIBROBLAST LINES

Human primary fibroblasts were acquired by skin punch biopsies or gingival explants under MSU-approved IRB protocols (ADF, E2F, EAF, and HSK). Commercial sources, including the ATCC (FET and HDNF) and the Coriell Institute (RET, SAF, and AUT), were also applied to the study. Additional information regarding these cell lines is located in Table 1 below. Mouse fibroblast lines were harvested from an individual, 5-month-old nu/nu mouse that was sacrificed by CO₂ overdose. The mouse carcass was disinfected with ethanol, and multiple tissues were removed for dissection. 125mm fragments of each target organ were removed and segmented. Individual tissue segments were placed in the wells of a six-well plate for outgrowth. Primary outgrowths were plated in fibroblast medium [Dulbecco's modified Eagle medium (DMEM), 10% fetal bovine serum (FBS), and 1 · antibiotic/antimycotic (Invitrogen)], and were then left undisturbed (excluding medium changes) for 2 weeks, and then passaged 1:1 to a new well. After an additional week of growth, the lines were passaged 1:2. This process was repeated to passage 5 at which time the wells were compared to positively identify those with typical fibroblast morphology, an absence of nonfibroblastic cells, and similar growth features. Thirteen mouse fibroblast lines were chosen for two additional rounds of passage and expansion. These cell lines were frozen as multiple aliquots for use in these experiments.

							Huma	an fibrob	last line	S										
General				mRNA expression											Immunocytochemistry					
Study ID	Line ID	Donor	Sex	Age	Tissue	COL1A2	FNECTIN	FIBR1	FIBU5	VIM	KER14	PECAM	FOXG1	SOX2	MYOD	MYF5	FNECTIN	VIM	SOX2	NEST
FET	IMR90	Healthy	F	E16 wk	Lung	+	+	+	+	+	-	-	-	-	-	-	+	+	-	-
NWB	HDNF	Healthy	M	Newborn	Skin	+	+	+	+	+	-	-	-	-	-	-	+	+	-	-
ADF	MSU-HUMGM	Healthy	M	44	Gingiva	+	+	+	+	+	-	-	-	-	-	-	+	+	-	-
RET	GM17880	Rett syndrome	F	5	Skin	+	+	+	+	+	-	-	-	-	-	-	+	+	-	-
E2F	MSU-HUMAG10	Healthy	M	73	Skin	+	+	+	+	+	-	-	-	_	_	_	+	+	-	_
EAF	MSU-HUMAG07	Healthy	M	71	Skin	+	+	+	+	+	_	-	-	_	-	_	+	+	-	_
SAF	GM01792	Schizophrenia	M	26	Skin	+	+	+	+	+	-	-	-	_	-	_	+	+	-	-
AUT	GM07992	idic(15) autism	F	3	Skin	ND	ND	ND	ND	ND	ND	ND	ND	ND	ND	ND	+	+	-	-
HSK	MSU-HUMSK	Healthy	M	41	Skin	ND	ND	ND	ND	ND	ND	ND	ND	ND	ND	ND	ND	ND	ND	ND

Table 1: General Properties of Fibroblast Lines. Study ID, abbreviated line designation used this report; Line ID, line common name; Donor, donor health status or strain; Sex, sex of donor (male, female, or of mixed sex); Age, age of donor (years, unless otherwise noted); Tissue, fibroblast tissue of origin. mRNA Expression: results of quantitative PCR analysis of multiple markers. COL1A2, fibroblast marker collagen type I alpha 2; FNECTIN, fibroblast marker fibronectin; FIBR1, fibroblast marker fibrillin I; FIBU5, fibroblast marker fibulin V; VIM, fibroblast marker vimentin; KER14, keratinocyte marker keratin 14; PECAM, endothelial cell marker Platelet endothelial cell adhesion molecule/CD31; FOXG1, neural progenitor marker Forkhead box protein G1; SOX2, neural progenitor marker SRY (sex determining region Y)- box 2, MYOD, myogenic progenitor marker MyoD1; MYF5, myogenic progenitor marker myogenic factor 5. Immunocytochemistry: summary of immunocytochemical analysis of fibroblast-associated

Table 1 (cont'd)

							Mous	e fibrobla	ast lines											
HE4	N/A	nu/nu	M	5 mo	Heart	-	+	+	+	+	-	-	-	-	-	-	+	_	-	-
SM1	N/A	nu/nu	M	5 mo	Skel Musc	+	+	+	+	+	-	-	-	-	-	-	+	+	-	_
K12	N/A	nu/nu	M	5 mo	Kidney	+	+	+	+	+	-	-	-	_	-	-	ND	ND	ND	ND
K13	N/A	nu/nu	M	5 mo	Kidney	-	+	+	+	+	-	-	-	-	-	-	+	+	-	-
K15	N/A	nu/nu	M	5 mo	Kidney	+	+	+	+	+	-	-	-	-	-	-	+	+	-	_
K16	N/A	nu/nu	M	5 mo	Kidney	+	+	+	+	+	_	_	-	_	_	-	+	+	_	_
LI6	N/A	nu/nu	M	5 mo	Liver	+	+	+	+	+	-	-	-	-	-	-	+	+	_	_
LU6	N/A	nu/nu	M	5 mo	Lung	+	+	+	+	+	-	-	-	_	-	-	ND	ND	ND	ND
TA4	N/A	nu/nu	M	5 mo	Tail Skin	+	+	+	+	+	_	_	-	_	_	-	+	+	_	_
TA6	N/A	nu/nu	M	5 mo	Tail Skin	+	+	+	+	+	-	-	-	-	-	-	ND	ND	ND	ND
TE4	N/A	nu/nu	M	5 mo	Testis	+	+	+	+	+	_	_	-	_	_	-	+	+	_	_
TE5	N/A	nu/nu	M	5 mo	Testis	+	+	+	+	+	_	_	_	_	_	_	+	+	_	_
LU3	N/A	nu/nu	M	5 mo	Lung	ND	ND	ND	ND	ND	ND	ND	ND	ND	ND	ND	ND	ND	ND	ND
MEF	N/A	FVB	F/M	E13 dy	Embryo	ND	ND	ND	ND	ND	ND	ND	ND	ND	ND	ND	ND	ND	ND	ND

(fibronectin, vimentin) and stem cell-associated markers (Sox-2, nestin) in fibroblast lines. N/A, not applicable; ND, –not done; +, positive; –, weakly positive; -, negative. (From Alicea et al. 2013 [54])

FIBROBLAST CHARACTERIZATION

Fibroblast RNAs from the mouse lines at passage 6–7 and the human lines at "passages" 8–10 were purified using Trizol (Invitrogen) or the RNeasy kit (Qiagen). Following the manufacturer's guidelines, 2 mg of purified RNA was converted to cDNA using Superscript II (Invitrogen). Quantitative polymerase chain reaction (qPCR) was executed on an ABI Prism 7000 analyzer using 1 mL of cDNA and normalizing against nuclear lamin A or ARHGAP mRNAs as internal controls. Other genes used as internal controls (RPL27A, EED, and GR) generated comparable results. Primers for qPCR analysis are shown below in Table 2.

PRIMER	5'-3' SEQUENCE	SPECIES
CLONING		
ASCL1 F	GAGAGAACGCGTGGCATGGAAAGCTCTGCC	Human
ASCL1 R	ACACACATCGATTCAGAACCAGTTGGTGAAGTCG	Human
MYF5 F	GAGAGAACGCGTATGGACGTGATGGATGGCTGCC	Mouse
MYF5 R	GTGTGTAATCGATTCATAGCACATGATAGATAAGCC	Mouse
MYF6 F	GAGAGAACGCGTATGATGATGGACCTTTTTGAAACTGG	Mouse
MYF6 R	GTGTGAATCGATTTACTTCTCCACCACTTCCTCCACGC	Mouse

Table 2:Primers Used in Cloning and qRT-PCR AnalysisPrimers Used in Cloning and qRT-PCR Analysis. Cloning- primers used in the amplification of cDNAs or plasmid DNA for construction of retroviral vectors; QPCR- primers used in qRT-PCR quantification of gene expression. The species of the gene targeted by each primer pair is shown on the right. (From Alicea et al. 2013 [54])

Table 2 (cont'd):

MYOD F	GAGAGAACGCGTGGTATGGAGCTTCTATCGCCGCCAC	Mouse
MYOD R	ACACACATCGATTCAAAGCACCTGATAAATCGC	Mouse
MYOG F	GAGAGAACGCGTATGGAGCTGTATGAGAC	Mouse
MYOG R	GTGTGTAATCGATTCAGTTGGGCATGGTTTCATC	Mouse
MYT1L F	GAGAGAGGCGCCCGATGGAGGTGGACACCGAGG	Human
MYT1L R	CACACAATCGATTCAGACCTGAATTCCTCTCACAGCC	Human
NEUROD1 F	GAGAGAACGCGTGGTATGACCAAATCGTACAGCG	Human
NEUROD1 R	GTGTGTGTTTAAACCTAATCATGAAATATGGCATTGAG CTG	Human
POU3F2 F	GAGAGAGGCGCCCAATGGCGACCGCAGCGTCTAAC C	Human
POU3F2 R	ACACACTATCGATTCAACGCGTCTGGACGGGCGTCTGC AC	Human
YFP F	CACAGGCCGCCTGGGCCATGGTGAGCAAGGGCG	Other
YFP R	AAACTTAACGCGTCTTGTACAGCTCGTCCATG	Other
ZIC1 F	GAGAGAGGCGCCCGGGAATGCTCCTGGACGCCGG	Human
ZIC1 R	ACACACATCGATTAAACGTACCATTCGTTAAAATTGGA	Human
Zierk	AGAGAGCGCAC	Taman
QPCR		
PANL27 F	CCATCCAGACTGAGGAAGACCCGGAAAC	Human/Mouse
PANL27 R	GGGCAGAAGCTCTGGTTCCTC	Hu/Mo
ARHGAP1 F	TGCTGTGGGCCAAGGATGCG	Human
ARHGAP1 R	GGTCCGGGCTTGGGAACAGC	Human
COL1A2 F	CAGGGGCTCTGCGACACAAGG	Human
COL1A2 R	TCCGGCTGGGCCCTTTCTTAC	Human
EED F	GGAAGGAGCCAGGAAGCCGC	Human
EED R	ACTGTCGCAAATCGCGCCCA	Human
FIBR1 F	AGGAAACCAGAGCCAGTCGGG	Human
FIBR1 R	GGAATGCCGGCAAATGGGGACA	Human
FIBU5 F	GTGTGTGAACCAGCCCGGCA	Human
FIBU5 R	ACGTCTGCAGGTTGCACG	Human
FNECTIN F	CGCCCTGGTGTCACAGAGGCTA	Human
FNECTIN R	TGGGGTGTGGAAGGGTTACCAG	Human
FOXG1 F	ACGGGGAGATCCCGTACGCC	Human
FOXG1 R	CCGCGAGCAGGTTGACGGAG	Human
KER14 F	GCAGCGGCCTGAGATCAA	Human
KER14 R	CATTGGCATTGTCCACTGTGGCT	Human
LAMIN F	GTGCGCTCAGTGACTGTGGTTGA	Human
LAMINR	CGAGCGCAGGTTGTACTCAGCG	Human
MYF5 F	TCTCCCCATCCCTCTCGCTGC	Human
MYF5 R	CCACTCGCGGCACAAACTCGT	Human
MYOD F	CTCCAACTGCTCCGACGGCA	Human
MYOD R	TCGACACCGCCGCACTCTTC	Human

Table 2 (cont'd):

PECAM F	TCCACATCAGCCCCACCGGA	Human
PECAM R	TGGGCCACAATCGCCTTGTCC	Human
SOX2 F	GGGGGAAAGTAGTTTGCTGCCTC	Human
SOX2 R	CTGCCGCCGATGATTGT	Human
VIMENTIN F	GAGCAGGATTTCTCTGCCTCTTCC	Human
VIMENTIN R	TCGTGATGCTGAGAAGTTTCGTTGA	Human
ARHGAP1 F	TTTGCCGAGCTTTGACAGGCG	Mouse
ARHGAP1 R	AATGGAGGCCAGCTTCAACTGG	Mouse
COL1A2 F	CAGGGGCTCTGCGACACAAGG	Human
COL1A2 R	TCCGGCTGGGCCCTTTCTTAC	Human
EED F	GGAAGGAGCCAGGAAGCCGC	Human
EED R	ACTGTCGCAAATCGCGCCCA	Human
FIBR1 F	AGGAAACCAGAGCCAGTCGGG	Human
FIBR1 R	GGAATGCCGGCAAATGGGGACA	Human
FIBU5 F	GTGTGTGAACCAGCCCGGCA	Human
FIBU5 R	ACGTCTGCAGGTTGCACG	Human
FNECTIN F	CGCCCTGGTGTCACAGAGGCTA	Human
FNECTIN R	TGGGGTGTGGAAGGGTTACCAG	Human
FOXG1 F	ACGGGGAGATCCCGTACGCC	Human
FOXG1 R	CCGCGAGCAGGTTGACGGAG	Human
KER14 F	GCAGCGGCCTGCTGAGATCAA	Human
KER14 R	CATTGGCATTGTCCACTGTGGCT	Human
LAMIN F	GTGCGCTCAGTGACTGTGGTTGA	Human
LAMINR	CGAGCGCAGGTTGTACTCAGCG	Human
MYF5 F	TCTCCCCATCCCTCTCGCTGC	Human
MYF5 R	CCACTCGCGGCACAAACTCGT	Human
MYOD F	CTCCAACTGCTCCGACGGCA	Human
MYOD R	TCGACACCGCCGCACTCTTC	Human
PECAM F	TCCACATCAGCCCCACCGGA	Human
PECAM R	TGGGCCACAATCGCCTTGTCC	Human
SOX2 F	GGGGGAAAGTAGTTTGCTGCCTC	Human
SOX2 R	CTGCCGCCGATGATTGT	Human
VIMENTIN F	GAGCAGGATTTCTCTGCCTCTTCC	Human
VIMENTIN R	TCGTGATGCTGAGAAGTTTCGTTGA	Human
ARHGAP1 F	TTTGCCGAGCTTTGACAGGCG	Mouse
ARHGAP1 R	AATGGAGGCCAGCTTCAACTGG	Mouse
COL1A2 F	CTCATACAGCCGCGCCCAGG	Mouse
COL1A2 R	CGGTTGGCTAGCAGGCGCAT	Mouse
EED F	CGCCGGCGGAACAGACATG	Mouse
EED R	TATTTGTGGGCGTGTCCGGGC	Mouse
FIBR1 F	AGGCCCCTGCAGTTACGGT	Mouse
FIBR1 R	CCTCGGCCCATGCCCATTCC	Mouse
FIBU5 F	ACAACCCGATACCCTGGTGCCT	Mouse

Table 2 (cont'd):

FIBU5 R	CGAGGCCCTTTGATGGGGCG	Mouse
FNECTIN F	GAGCGACATGCTCTACAAAGTGCT	Mouse
FNECTIN R	CTGGGGGTGAGTCTGCGGTTG	Mouse
FOXG1 F	CGATCGCGGCTACCGGCTTC	Mouse
FOXG1 R	CACTCCCAGAGTCGCGCTCAC	Mouse
KER14 F	ACAGCCCTACTTCAAGACCATCG	Mouse
KER14 R	CGCAGGCTCTGCTCCGTCTC	Mouse
LAMIN F	GCCTTCGCACCGCTCTCATC	Mouse
LAMINR	GCCGCTGCAGTGGGAACC	Mouse
MYF5 F	CCCCAACCTCAGCCACTGACC	Mouse
MYF5 R	GCCAGCAAATCCAGGCGGAGC	Mouse
MYOD F	GGAGATCCTGCGCAACGCCA	Mouse
MYOD R	GCAGCGGTCCAGGTGCGTAG	Mouse
PECAM F	ACGAGAGCCACAGAGACGGTG	Mouse
PECAM R	AGGGACGTGCACTGCCTTGAC	Mouse
SOX2 F	GCTGCCTCTTTAAGACTAGGGCTG	Mouse
SOX2 R	GCCGCCGATTGTTGTGAT	Mouse
VIMENTIN F	GTCGAGGTGGAGCGGACAAC	Mouse
VIMENTIN R	CCGTTCAAGGTCAAGACGTGCCA	Mouse

Human and mouse fibroblasts were processed for immunocytochemical analysis to inspect marker expression at the individual cell-level, following the methods described below for iNC analysis. Primary antibodies were applied to the experiment as follows: anti-vimentin 1:1250 (Millipore AB5733), anti-fibronectin 1:750 (BD, 610077), anti-nestin 1:250 (Santa Cruz Biotechnologies;H-85), and anti-Sox2 1:250 (Santa Cruz Biotechnologies; Y-17). Multiple images of each immunostained line were gathered. Approximately 1x10³ cells were inspected at high magnification for the presence or absence of those markers consistent with stem cell (Sox-2/nestin) or fibroblast identity (vimentin/fibronectin). Neural progenitor cells (NPCs) used for comparison were fixed in parallel with fibroblasts, and were generated as described below for iNC analysis.

The relative infectivity for factor expression was calculated by infecting 1x10⁵ actively growing cells with concentrated NITSC-NLS-YFP retrovirus at an MOI of approximately 0.5. 4

days post-infection, the yellow fluorescent protein (YFP) positive cells were counted as a fraction of all cells over three replicates. The precise cellular age of each cell line was partially unknown. Therefore, verification was required to confirm that none of the analyzed lines were approaching cellular senescence, which could influence the reprogramming process.

During the verification procedure, each line was continuously passaged and counted for four rounds (post-experiments) to confirm that all lines were still actively proliferative. One of the 13 mouse lines, LU3, stopped proliferating by the third trial passage and was removed from the final analysis. Two human lines, AUT and HSK, produced iNCs that were partially characterized, but were not included in the final analysis. Prior to completion of various experiments, the laboratory experienced freezer failure, resulting in the loss of "matching" frozen stock. Similarly, mouse lines TA6, KI2, and LU6 were not included in the experiments shown in Figure 2 due to freezer failure.

INC INDUCTION

cDNAs encoding human ASCL1, POU3F2, and ZIC1 were obtained from Open Biosystems. Myt1L and NeuroD1 open reading frames (ORFs) were obtained from cDNA produced from human brain reference RNA (Applied Biosystems). NITSC was produced by introducing the BstEII-ClaI fragment encompassing Neo-IRES-TTA-TetO from NIT (GenbankAcc# AF311318) into BstEII-ClaI cut pMSCVneo (Clontech) and a polylinker for transgene expression, SfiI-MluI-PmeI-ClaI. Primers used for cloning factors into NITSC are shown in Table 2. The amplified YFP ORF with a MluI site inserted immediately prior to the stop codon was digested with SfiI-PmeI and introduced into NITSC to produce the control vector NITSC-YFP. Remaining factor ORFs were polymerase chain reaction (PCR) amplified with compatible MluI or Asc1 sites at the 5' end and ClaI at the 3' end for cloning into NITSC-YFP

to create the fusion protein constructs. NITSC recombinant moloney murine leukemia virus (MMLV) particles were made by three-way calcium phosphate transfection of Human Embryonic Kidney 293 (HEK) cells with gag-pol and Vesicular stomatitis virus (VSV) encoding plasmids to produce replication defective virus particles. Two days post-transfection, viral supernatants were harvested, filtered and introduced into fibroblast cultures via the carrier polybrene (8 mg/mL) to increase infection efficiency as described for lentiviral vectors in Suhr et al. [34]. Viral supernatants were frozen as aliquots and used on mouse embryonic fibroblasts (MEFs) to provide a rough titer, and to allow viral preparations to produce iNCs before use with target cells. The YZIC/YASCL/YPOU3F (ZAP) combination appeared the most potent on both mouse and human fibroblasts in preliminary experiments, and was used for conversion unless otherwise noted. Equal volumes of each viral supernatant were applied (i.e., for ZAP, typically 5mL of each viral supernatant for a total of 15mL infectious medium/ 10-cm plate).

In order to determine the superlative conditions for iNC conversion during preliminary studies, approximately $1x10^6$ mouse or human fibroblasts (growing in fibroblast medium at equal confluency) were infected with viral medium followed by an overnight wait-period to allow for infection. Virus-infected cultures were then passaged by trypsin treatment to six-well, 12-well, or 35mm tissue culture plates followed by a period of 12-24 hours in fibroblast growth medium to support plate attachment and cellular growth. The fibroblast medium was then aspirated and replaced with iNC medium (DMEMF12 with N2 supplement and penicillin/streptomycin at 50 m/mL) (Invitrogen). The iNC medium was changed at 4–5 day intervals for the duration of the experiment, and the cells were kept in a 5% CO₂ environment at 37° C. Cell culture plates coated with polyornithine/laminin (PORN/lam), or without coating,

were used for preliminary experiments interchangeably with little noticeable impact on the formation of iNCs.

To determine the optimal time for counting iNCs, factor-infected MEFs and adult mouse and human fibroblast cultures were fixed and immunostained with the neural TUJ1 antibody at 5–6 day intervals post-infection. iNC conversion (for the purpose of reprogramming efficiency across mouse and human cells lines) was executed fundamentally as described previously.

However, 1x 10⁶ target cells in one well of a six-well plate were infected with 3mL of the iNC (ZAP) viral mixture and 24 hours later, passaged to three wells of a 12-well plate. The passaged cells were allowed to rest an additional day, followed by a transition to iNC medium.

Subsequent medium changes occurred every 3–4 days until fixation and immunoprocessing on day 12 for mouse iNCs and day 24 for human iNCs. Experiments for quantification of reprogramming efficiency were performed in three distinct replicates.

IMMUNOHISTOCHEMISTRY AND IMAGING

Cells were fixed with 4% paraformaldehyde for 10 minutes followed by 3 phosphate-buffered saline (PBS) washes for 10 minutes each. PBST (PBS with 0.3% Triton X-100) with 3% donkey serum (DS) was used for 30–60 minutes at room temperature to block, and was then replaced with PBST + 1% DS containing added primary antibody overnight at 4° C. The primary antibodies were used at the following dilutions: TUJ1-1:3000 (Santa Cruz; Cat# sc-58888), MAP2ab - 1:300 (Sigma; Cat#M1406), Synapsin 1–1:400 (Millipore; Cat#AB1543P), panneurofilament–1:1000 (Covance; SMI311), Doublecortin–1:400 (Santa Cruz, Cat#sc-8066), GAD–1:250 (Santa Cruz; Cat#sc-7513), PSD95–1:250 (NeuromAb), and GABAR3–1:250 (NeuromAb). After incubating overnight with the primary antibody, wells were washed with PBST + 1%DS 3 times for 10 minutesand incubated with PBST + 1%DS with the

applicablesecondary antibody (JacksonImmunoResearch) for 30–60 minutes. Wells were subsequently washed with PBS 3 times for 10 minutes to remove excess secondary, stained briefly with PBS + 1 mg/mL bis-benzamideto label nuclear DNA, and then rinsed again. All plates and wells were held at 4° C in the dark until imaging procedures were completed on a Nikon Eclipse TE2000 inverted stage fluorescence microscope.

ELECTROPHYSIOLOGY

Infected NPC neurons or iNCs were cultured on PORN/lam-coated 35mm plates at a low density (2.5×10^5) cells/35mm plate) as described previously for electrophysiological recordings. All recordings obtained were generated using the entire cell configuration of the patch-clamp technique [35]. The patch glass pipette electrodes were double pulled and heat polished. The electrode was brought into contact with visually identified iNC targets to produce a highresistance seal between electrode tip and the cell membrane. The entire cell configuration was attained by applying suction to the back of the electrode. For voltage clamp experiments, electrode capacitance was compensated before attaining the whole cell configuration, and membrane capacitance and series resistance were compensated after accomplishing this configuration. Membrane current and potential signals were amplified (List Electronic EPC-7), digitized (Digidata 14140A; Molecular Devices), and recorded on a computer. Voltage steps and current injection pulses were generated and potential and current signals were evaluated using software written by Dr. John Dempster (Dept. Physiology, University of Strathclyde). In every voltage clamp recording, the holding potential (Vh) was - 80 mV. The existence and properties of voltage gated current was analyzed during positive voltage steps (30 to 250 ms depending on the experiment) to test potentials (Vtest) between - 75mV and + 50 mV. To inspect voltage dependent, steady-state inactivation of voltage gated Na+ channels, a double voltage step

was used: A step to a conditioning potential (Vcon, - 130mV to + 40 mV, 50 ms) was applied directly before the step to the test potential (0 mV). To evaluate whether or not cells had the ability to produce action potentials, membrane potential was measured under current clamp.

The extracellular solution used was comprised of NaCl 135mM, KCl 5mM, glucose 10mM, MgCl2.6H2O 1mM, CacCl2.2H2O 2mM, and HEPES 20mM (pH 7.3). The recordings of isolated voltage-gated Na+ current, the electrode solution comprised of CsCl 20mM, cesium methanesulfonate 130mM, MgCl2.6H2O 2mM, glucose 10mM, EGTA 10mM, and HEPES 10mM (pH 7.3). The recordings of mixed voltagegated Na+ and K+ current, and for the recordings of membrane potential and action potentials, the electrode solution comprised of KCl 20mM, potassium methansulfonate 130mM, MgCl2.6H2O 2mM, glucose 10mM, EGTA 0.01mM, and HEPES 10mM (pH 7.3).

HUMAN NPC CULTURE AND NEURON DERIVATION

For the control human neurons shown in Figure 1 below, H9 human ES cells were differentiated to NPCs as described in[36]. H9-NPCs were propagated to passage 5 in iNC medium with 20 ng/mL FGF-2 added.NPCs were plated on PORN/lam plates, and FGF-2 was gradually withdrawn to a final concentration of 2 ng/Mlby day 20–24 for differentiation. Cells were then processed for immunostaining confirm neuronal identity and electrophysiological analysis was performed. As controls in the experiments undifferentiated NPCs at 30%–50% confluencywere fixed and used as shown below in Figure 2.

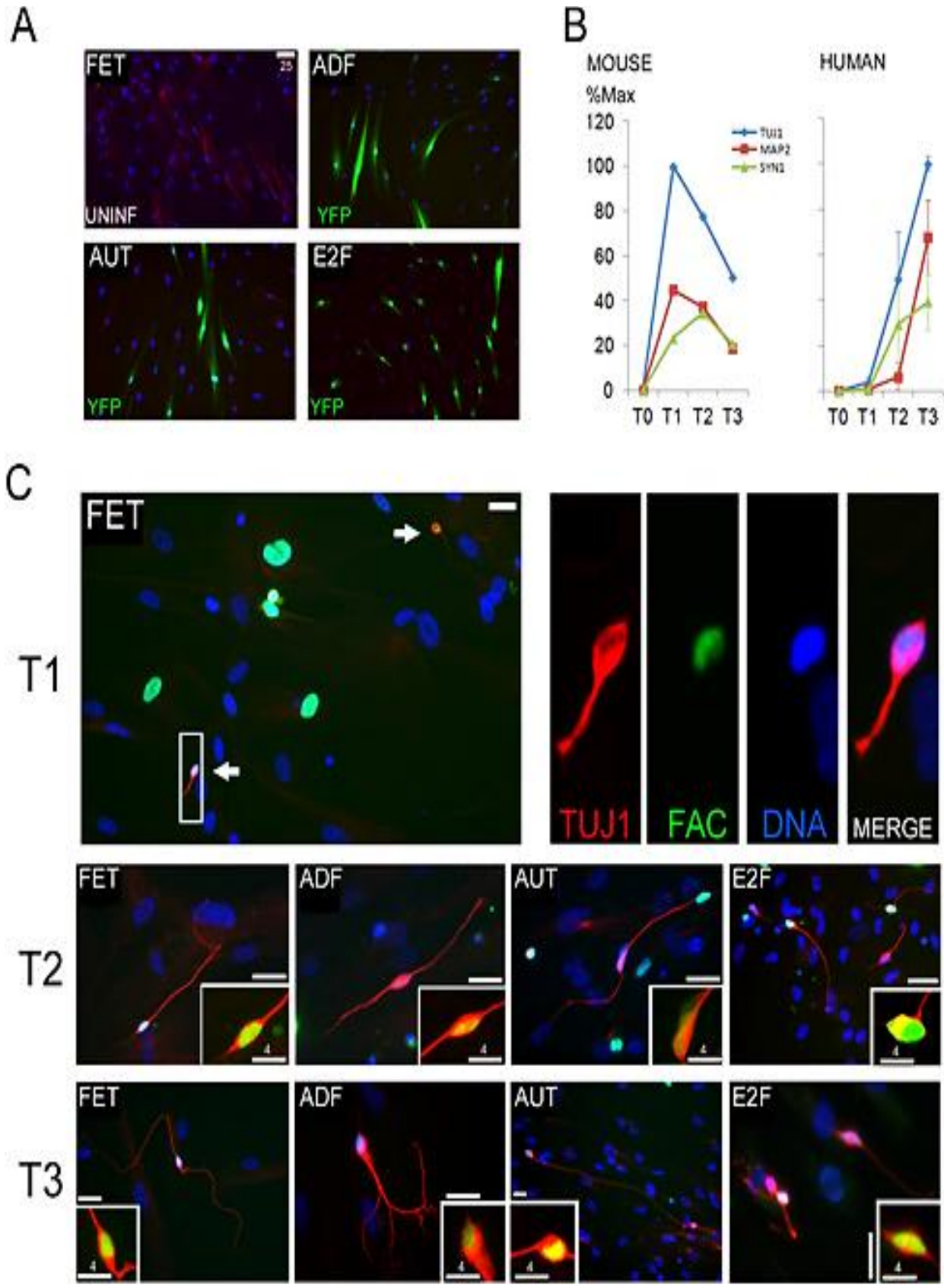


Figure 1: Time Course of induced Neural Cell (iNC) Induction and Electrophysiological

Figure 1 (cont'd):

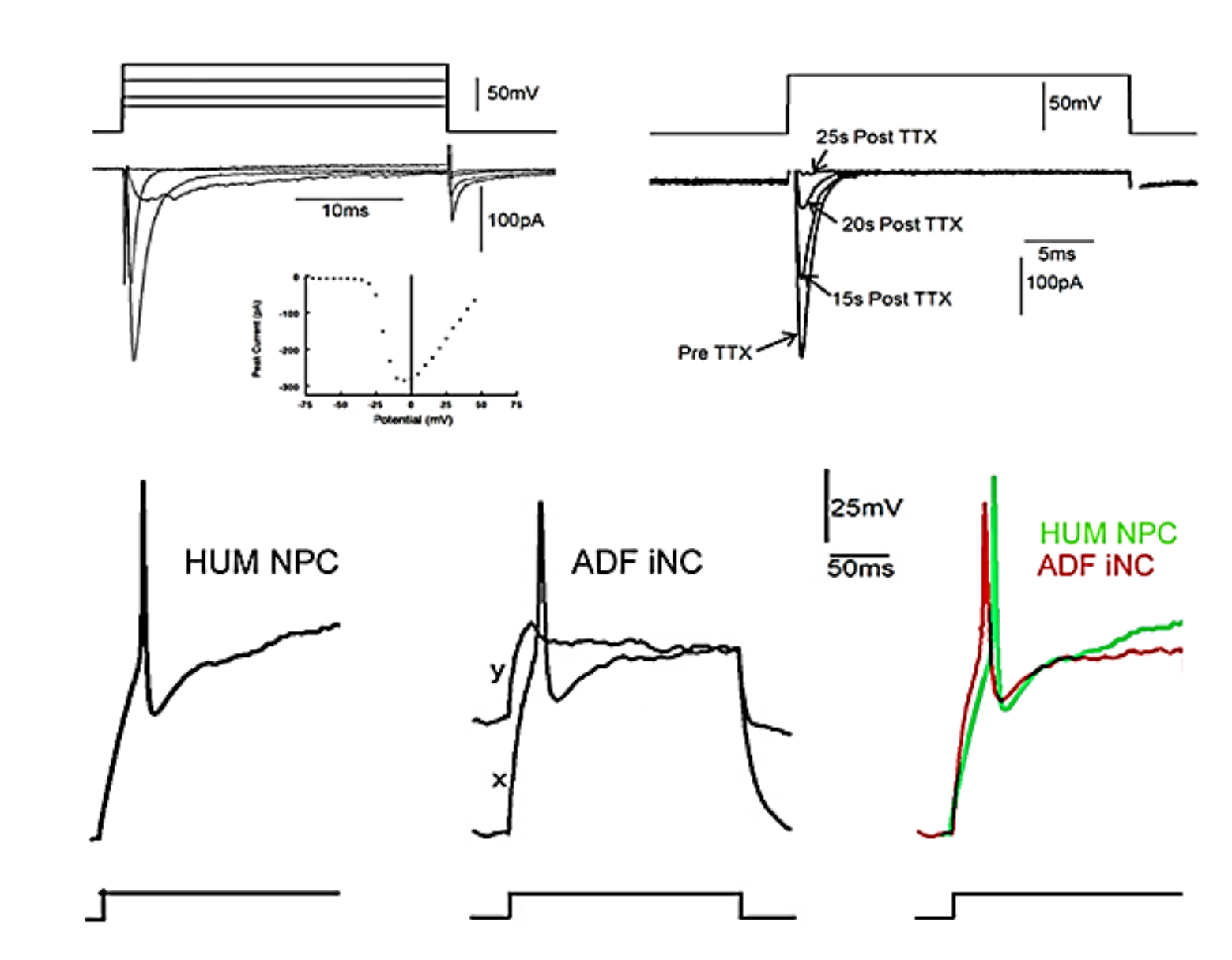


Figure 1 (cont'd): Analysis. (A) Examples of untransduced fibroblasts or fibroblasts infected with a YFP-only control vector (green) cultured under INC induction conditions for 4 weeks and stained for TUJ1 (red). (B) TUJ1-, SYN1-, and MAP2-positive mouse and human iNCs over time expressed as a percentage of the maximum TUJ1 value. Infection was at time 0 (T0), T1 = 8–10 days, T2 = 18–20 days, and T3 = 28–30 days. BLUE: TUJ1, RED: MAP2, GREEN: SYN1. (C) Examples of human iNCs produced by different fibroblast lines at the T1-T3 time points (labeled on left) and stained for TUJ1 (red). In the upper left panel, arrows indicate early iNCs in a low-magnification field. In the upper right panel, the iNC boxed At the left is shown magnified for each color channel and the merged image. In the center and lower panels, iNCsatthe T2 and T3 time points, respectively, are shown. Scale bars are 10 mm unless otherwise noted. Insets depict the cell soma with the blue channel removed to more clearly reveal iNC factor expression. (D) Representative electrophysiological recordings from iNCs. Upper left panel - Isolated voltage-gated sodium current recorded from a representative human iNC. Upper records show voltage steps from a holding potential of - 80mV to test potentials of - 40, - 25, 0, and 25 mV. Lower records show leak-subtracted Na + current elicited by these voltage steps. Note that the step to - 40mV is sub threshold and that the steps to - 25, 0 and 25mV are supra-threshold and elicit inward sodium current of amplitude and kinetics which is voltage dependent. Inset shows the relationship of test potential and the maximum amplitude of the Na + current elicited at each test potential in this cell. Upper right panel—Voltage-gated inward Na+ current was blocked by TTX. Upper record: voltage step from - 80 to 0 mV, which was repeated every 2.5 s during the recording. Lower records: current elicited by the membrane depolarization at different times during the recording. Voltage-gated inward Na+ current (but not outward K+ current) was reduced in a time-dependent manner after the application of TTX (5 mM) to the extracellular medium. Lower panels—Representative action potentials (APs) recorded from NPC-neurons and INCs. Left - AP produced by an NPC-derived neuron. Membrane potential change (upper record) elicited by application of membrane current step (lower trace) while holding the membrane at - 72mV just before current step application. Center—AP produced by an ADF iNC. Membrane potential changes (upper records, x and y) elicited by application of membrane current step (lower trace) without (x) and with (y) holding the membrane at - 90mV (x) or -55mV (y) just before current step application. Right—Overlay of the NPC and INC AP traces (NPC, green; ADF, red). Top Panel: Raw tracings for visual reference only. (From Alicea et al. 2013 [54]) For interpretation of the references to color in this and all other figures, the reader is referred to the electronic version of this thesis.

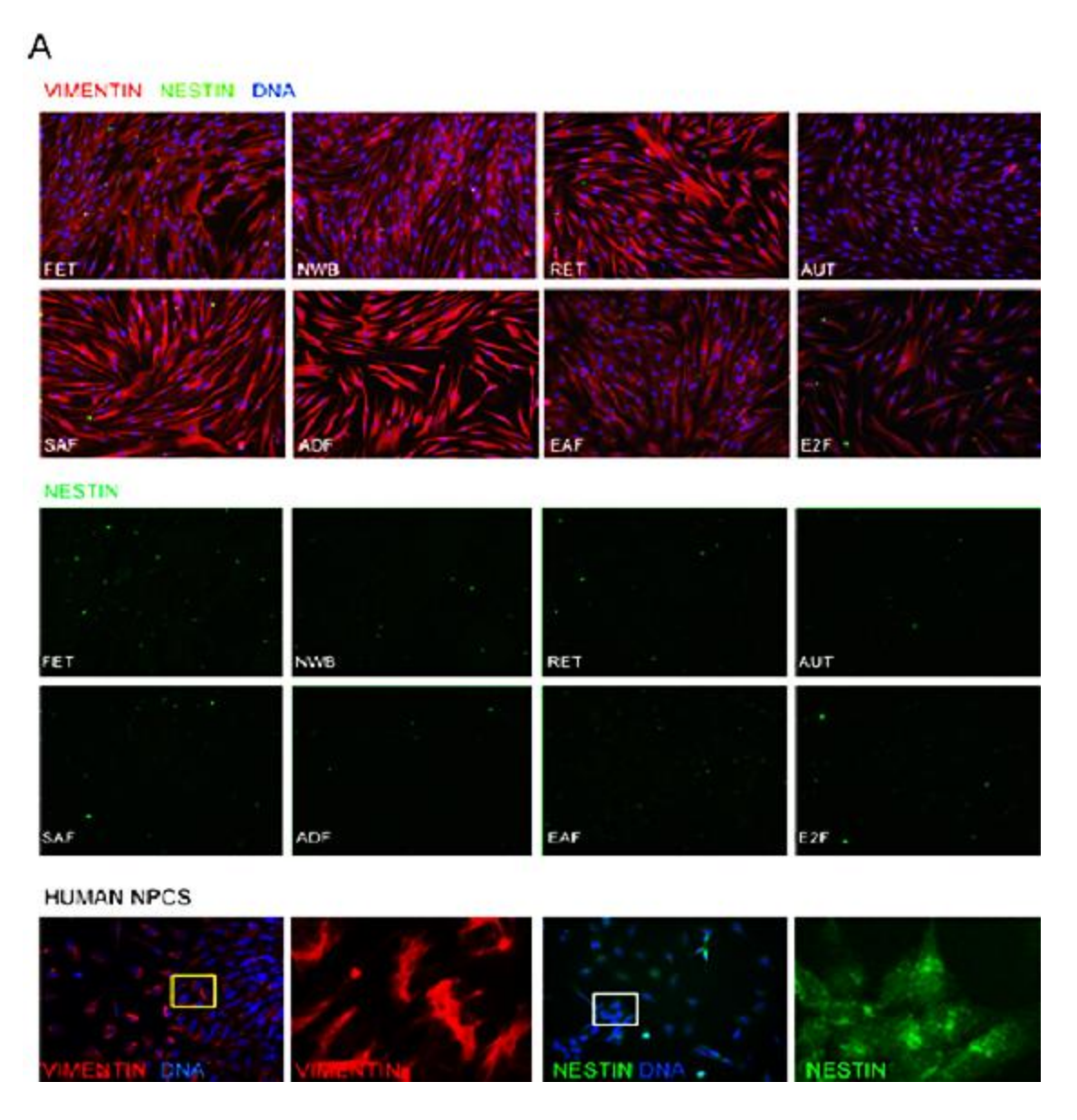


Figure 2:Immunocytochemical Examination of Mouse and Fibroblast Lines.(A,B) Mouse fibroblast lines analyzed for immunocytochemical components. The panels at the end show that as with human cells, rare patches of dim green fluorescence do not co-localize with nuclei and do not indicate Sox-2 immunoreactivity. Blue color in all images is nuclear DNA stain bisbenzimide. (C) Anti-fibronectin (red) and anti-Sox2 (green) antibodies. Insets in middle panels display magnified images, demonstrating that rare spots of dim green fluorescence are not cell/Figure 2 (cont'd): nucleus associated as with genuine Sox-2 immunopositivity observed in NPCs. (D) Immunostaining of human cell lines with anti-vimentin (red) and anti-nestin (green) antibody. Upper panels—both antibodies in all fibroblast cell lines. Middle panels—the green channel only (nestin), exhibiting an absence of positive signal. Lower panels --- controls demonstrating the same antibodies on human NPCs as labeled.(A) Top Legend (Left to Right): VIMENTIN NESTIN DNA. DATA (Left to Right): FET, NWB, RET, AUT, SAF, ADF, EAF, E2F. Middle Legend: NESTIN. DATA (Left to Right): FET, NWB, RET, AUT, SAF, ADF, EAF, E2F. Bottom Legend: HUMAN NPCS. DATA (Left to Right): VIMENTIN DNA,

Figure 2 (cont'd):

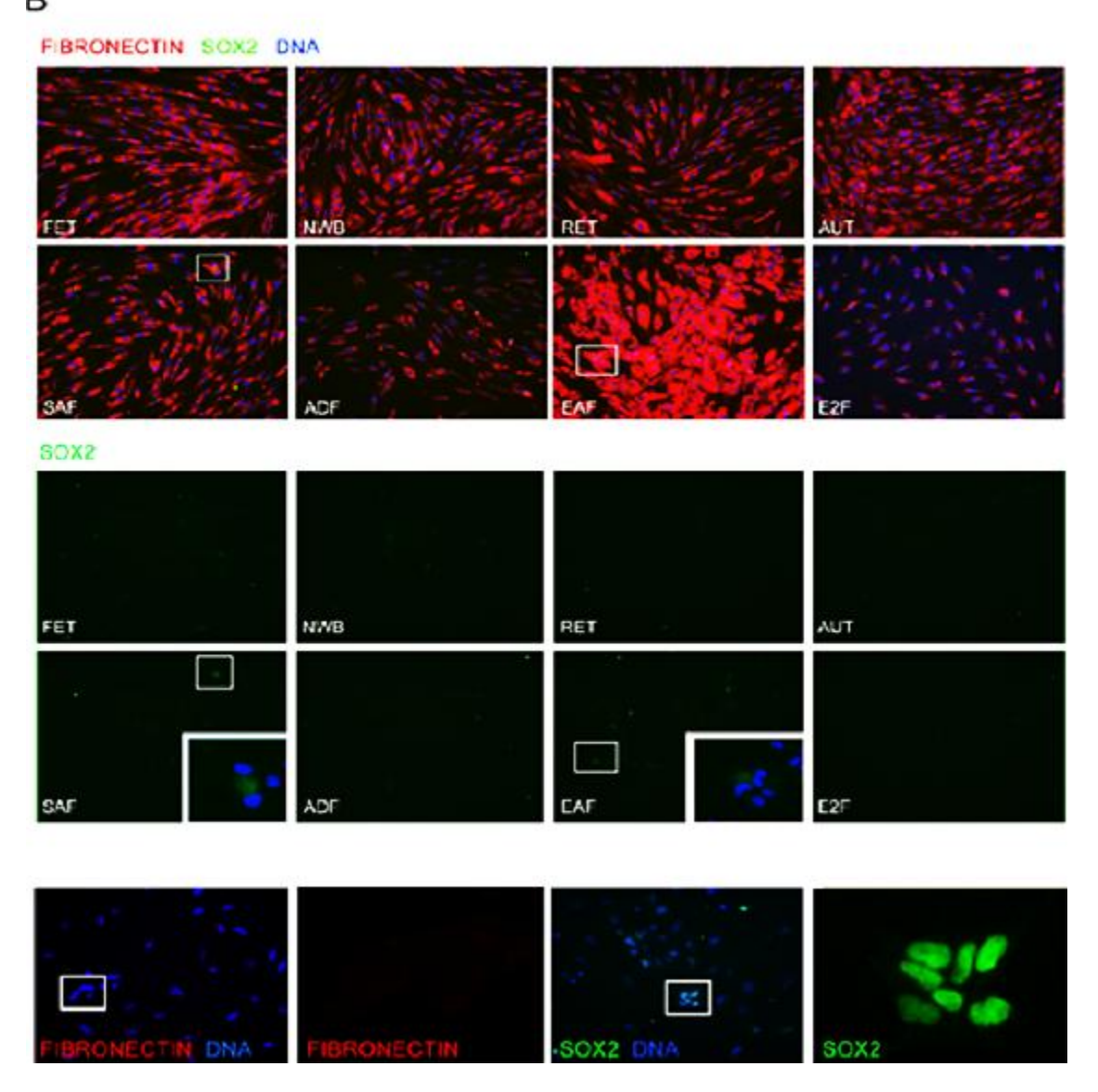


Figure 2 (cont'd):

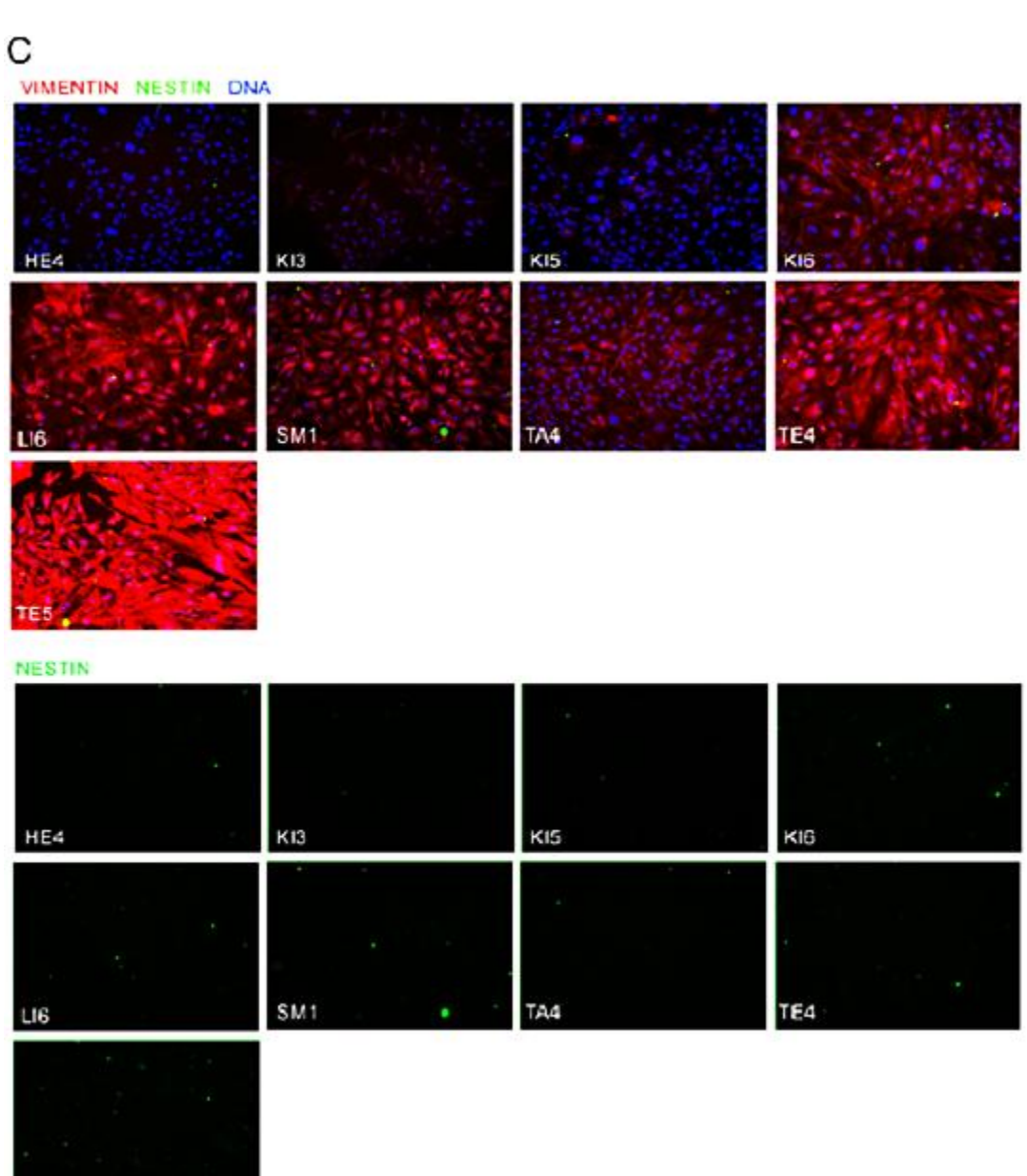
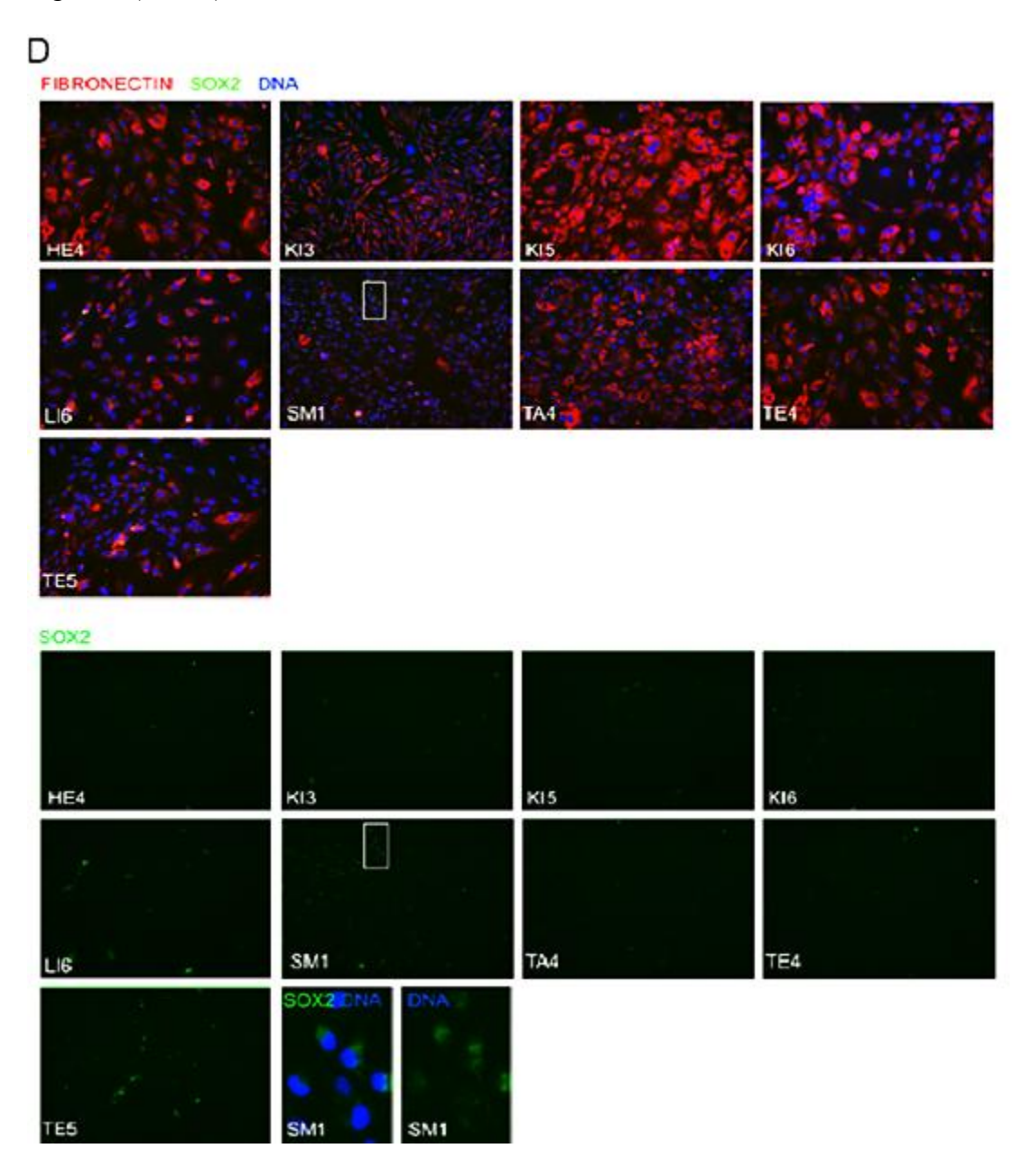


Figure 2 (cont'd):



VIMENTIN, NESTIN DNA, NESTIN. B) Top Legend (Left to Right): FIBRONECTIN SOX2 DNA. (Left to Right): FET, NWB, RET, AUT, SAF, ADF, EAF, E2F. Middle Legend: Sox2. DATA (Left to Right): FET, NWB, RET, AUT, SAF, ADF, EAF, E2F. Bottom Data (Left to Right): FIBRONECTIN DNA, FIBRONECTIN, SOX2 DNA, SOX2. C) Top Legend (Left to Right): VIMENTIN NESTIN DNA. Data (Left to Right): HE4, KI3, KI5, KI6, LI6, SM1, TA4, TE4, TE5. Middle Legend: Nestin. Data (Left to Right): HE4, KI3, KI5, KI6, LI6, SM1, TA4, TE4, TE5. Bottom Legend: Data (Left to Right): HE4, KI3, KI5, KI6, LI6, SM1, TA4, TE4, TE5.D) Top Legend: (Left to Right): FIBRONECTIN SOX2 DNA. Data (Left to Right): HE4, KI3, KI5, KI6, LI6, SM1, TA4, TE4, TE5. Bottom Legend: SOX2 Data (Left to Right): HE4, KI3, KI5, KI6, LI6, SM1, TA4, TE4, TE5.

QUANTIFICATION OF INC CONVERSION

Quantification of iNC conversion was accomplished by using Hoechst33342 staining for nuclei/DNA (Blue), YFP fluorescence of the tagged proteins to indicate relative factor expression (Green), and β-IIITubulin/TUJ1 (iNCs) immunostaining to indicate phenotypic conversion (Red). Relative reprogramming efficiency was calculated by dividing the red fluorescence value by the blue fluorescence or by dividing the red/blue value by the green fluorescence value to contain a factor-expression component in the calculation. iNC conversion was measured as the number of red fluorescent cells that had fibers of at least three soma lengths. For each well, five fields were imaged at 100X magnification for each separate channel and stored as a merged RGB image. The fields included one in the center of each well, and one at each compass point (approximately 1 cm from the well edge). To measure fluorescence, the RGB image was separated into individual black and white channels followed by quantification with NIH ImageJ. The highest relative conversion value for iNCs for each group was set at 100 in the graphs, and the remaining values were calculated as a fraction of that maximum.

RESULTS

In an attempt to limit technical variance, all procedures were performed in parallel on all cell lines within a group with a minimum of three distinct experiments. Fibroblasts were selected as the input cell type for a variety of reasons. Fibroblasts are naturally adherent and capable of undergoing cryogenic preservation. Furthermore, the ability of fibroblasts to be passed and established with little difficulty has been previously recognized, and these cells have been used in many studies published by various authors reporting a large variance of reprogramming efficiency to a desired output cell type. Human fibroblasts were selected as an input cell type due to their ability to be directly translated into clinical application for human medicine. An

assortment of ages was selected for human fibroblasts with numerous older subjects due to a higher probability for older subjects to serve as the primary target for cellular reprogramming-based therapy. Mouse fibroblasts were selected as an input cell type because all lines were derived from a single donor, therefore being isogenic, and multiple lines could be harvested from the same isogenic organ for comparison. As illustrated below in Figure 3, human and mouse fibroblasts lines were grown in cell culture, underwent over eight passages while still exhibiting homologous morphology, and were a minimum of four passages from mitotic senescence.

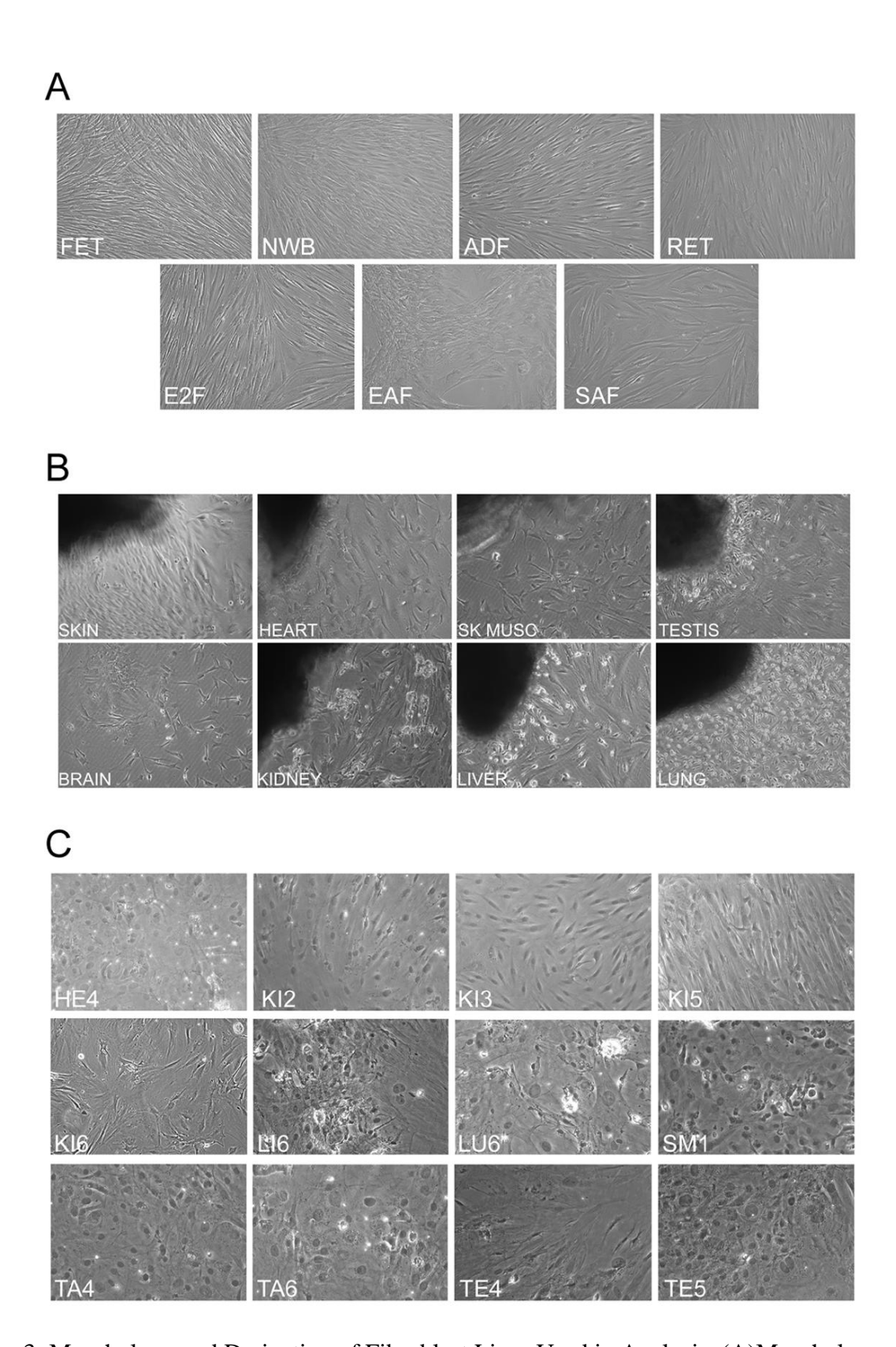


Figure 3: Morphology and Derivation of Fibroblast Lines Used in Analysis. (A)Morphology of

Figure 3 (cont'd): the seven human fibroblast lines used for analysis. (B) Outgrowth of fibroblasts and other cell types from tissue fragments of eight mouse tissues at 1 week post plating. The dark mass in the upper left corner is the adherent tissue fragment itself. (C) Morphology of the twelve mouse fibroblast lines (at passage 6) used for analysis. (From Alicea et al. 2013 [54])

Quantitative real-time polymerase chain reaction (RT-PCR) analysis was performed to confirm an abundance of fibroblast-associated mRNAs, and the absence of significant signals for indicators of other differentiated or progenitor cell types as illustrated below in Figure 4. All fibroblast lines displayed an abundance of the fibroblast-associated markers collagen type 1α2, vimentin, fibronectin, fibrillin I, and fibulin V with mouse lines HE4 and KI3 testing negative for mouse collagen type 1α2. HE4 also displayed weak vimentinimmunopositivity, but immunopositivity none the less. Because both lines were positive for most fibroblast markers, and negative for stem cell type mRNA indicators, both lines remained in the study. mRNAs for other common contaminating cell types such as keratinocytes and endothelial cells were not detected via RT-PCR displayed on both Table 1 and Figure 4.



Figure 4:Fibroblast- and Nonfibroblast-associated mRNA Expression in Human and Mouse Fibroblast Lines. Heat map color is

Figure 4 (cont'd): proportional to expression level—bright green is high expression and black is no detectable transcript.COL1A2, collagen type 1a2; FNECTIN, fibronectin; FIBR1, fibrillin I; FIBU5, fibulin V; KER14, keratin 14.(From Alicea et al. 2013 [54])

Immunohistochemical analysis of fluorescence for Sox-2 and nestin was performed to further characterize the fibroblasts at the individual cell level of each line. These markers are not expressed at significant levels in fibroblast [37-43], however they are expressed robustly in multiple stem cell classes including neural stem cells. As demonstrated in Figure 2 and summarized in Table 1, no cells displayed immunopositivity for either stem cell marker nestin or Sox-2.

iNCs were chosen as the output cell type due to reports of successful direct reprogramming from multiple laboratories using similar protocols [15, 44-47]. Also, conversion can be measured by morphological changes and functional changes divergent from input fibroblast characteristics, therefore making conversion easily identifiable. For iNC conversion, all fibroblasts were infected in parallel with combinations of an MMLV-based retroviral vector encoding the neurogenic transcription factors ASCL1, POU3F2, ZIC1, MYT1L, or NeuroD1 [15,45] of human origin fused to YFP as shown schematically below in Figure 5.

NITSC-YFP-X

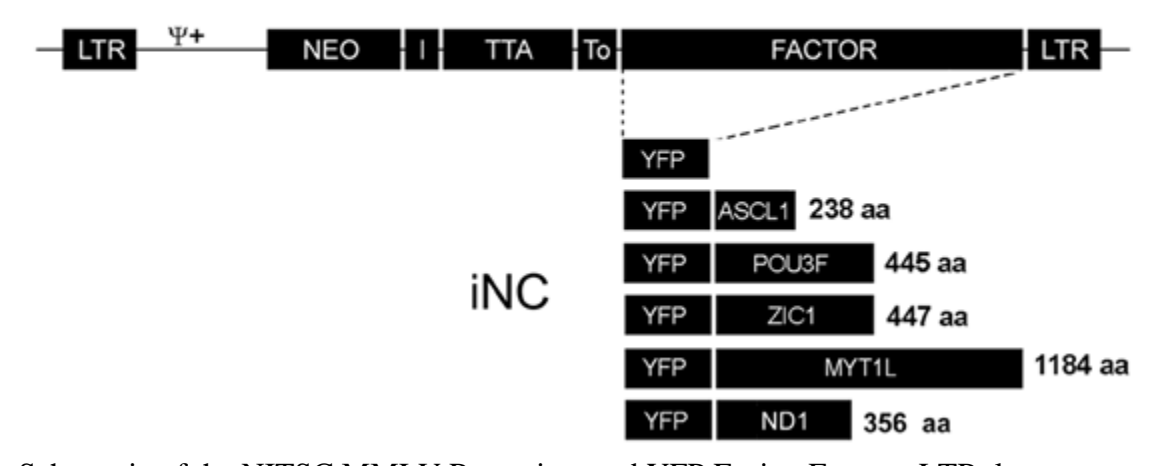


Figure 5: Schematic of the NITSC MMLV Retrovirus and YFP Fusion Factors. LTR, long

Figure 5 (cont'd):terminal repeat; Ψ^+ , stem-cell permissive packaging sequence; NEO, G418-resistance gene; I, IRES element; TTA, tet-transactivator; To, tetoperator.(From Alicea et al. 2013 [54])

YFP-fusion proteins localized primarily to the nucleus (Figure 6A). Cells infected with a YFP vector only and cultured under identical conditions (used as a control) produced no strongly TUJ1-positive cells or displayed neuron-like morphology (Figure 6A). Cells infected with ASCL1, POU3F2, and ZIC1 transcription factors alone generated very small amount of iNCs (Figure 6B, upper panel) whereas a combination of ASCL1, POU3F2, and ZIC1 generated many TUJ1-positive iNCs for both human and mouse fibroblasts lines (Figure 6B, lower panel and Figure 7).

The primary difference between the generation of mouse and human iNCs was the maturation rate [15, 44-47]. Mouse iNCs reached mature morphology by day12 post-infection, whereas human iNCsreached mature morphology at day 24 post-infection. Mature iNCs that displayed processes greater than three cell body lengths were selected to be indicative of mature neurons. The criterion of three soma-lengths as an indicator of bona-fide iNCs was originally described by Vierbuchen et al. [15], and is based on the observation that iNCs with fibers of this length or greater frequently also expressed multiple markers associated with mature neurons. In our human and mouse iNCs displaying long processes, mostwere positive for multiple markers of mature neurons in addition to TUJ1, including MAP2a/b, synapsin 1, doublecortin, neurofilament 300 kDa as shown in Figure 6C and Figure 6D.iNCs also exhibited electrophysiological properties such as TTX-sensitive Na+ currents and action potentials that were essentially indistinguishable from human neurons generated under identical conditions from human ES cell-derived human neural progenitor cells (NPCs) analyzed via patch clamp analysis (Figure 1D).

Maximum conversion efficiency (calculated by percent of output cells versus unconverted cells) for mouse fibroblasts to iNCs was 0.72% – 0.08% (TA4), and 1.07% – 0.18% for human cells (RET). This is lower than some other published studies that reported 2%–18% conversion using the same or different combinations of factors [15,44–46]; however, the lower efficiency maybe caused by using YFP-linked transcription factors. Reprogramming efficiency was calculated by dividing the red fluorescence value (iNC conversion indicated by TUJ1 immunostaining) by the Hoechst 33342 fluorescence value (indicating stained nuclei), as shown in Figure 6 E and F. As demonstrated in this figure, there was a wide array of reprogramming efficiency among different cell lines, even in mouse cell lines that were isogenic and in some cases from the same organ (i.e. the KI cell lines).

A

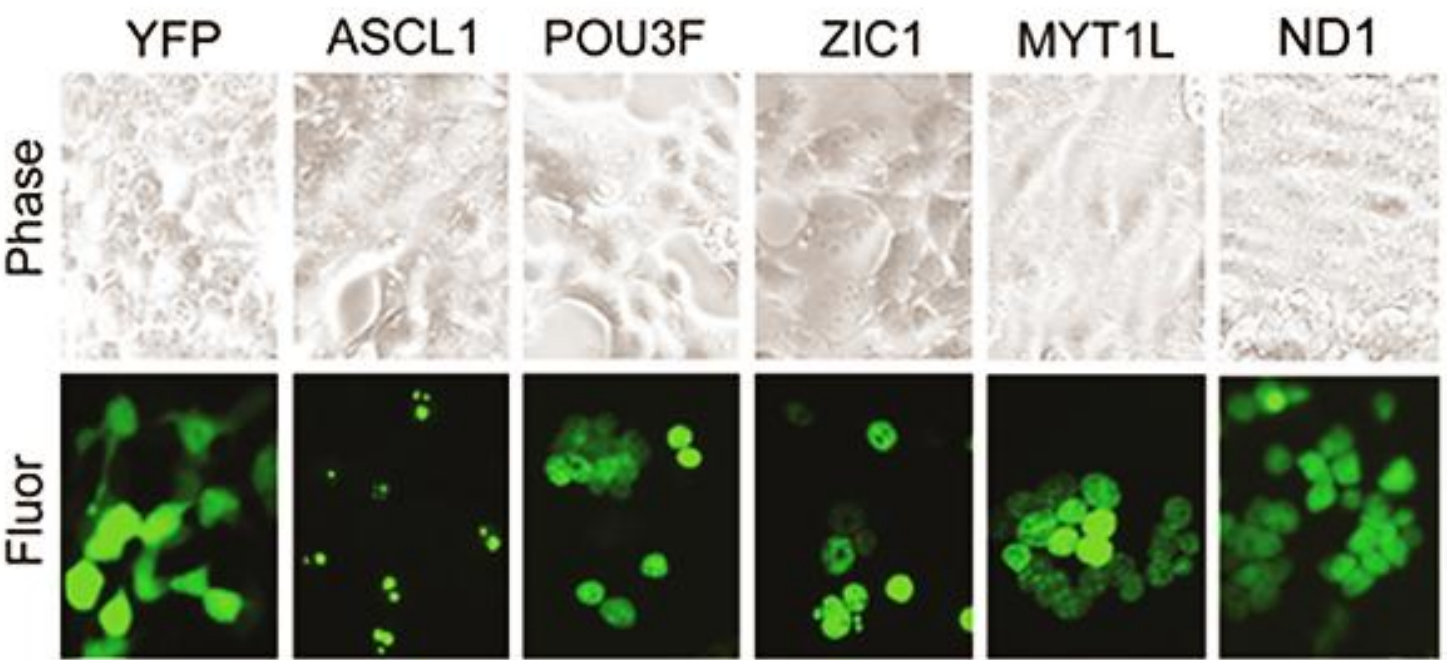


Figure 6: Figure 6: Induced Neural Cell (iNC) Conversion of Mouse and Human Fibroblast Lines. (A) HEK cells transfected with YFP fusion protein for iNC conversion, as labeled. Phase-contrast images are in the upper panels, and corresponding fluorescent images are in the lower panels. (B) Mouse embryonic fibroblasts infected with the individual factors (as labeled) and stained for

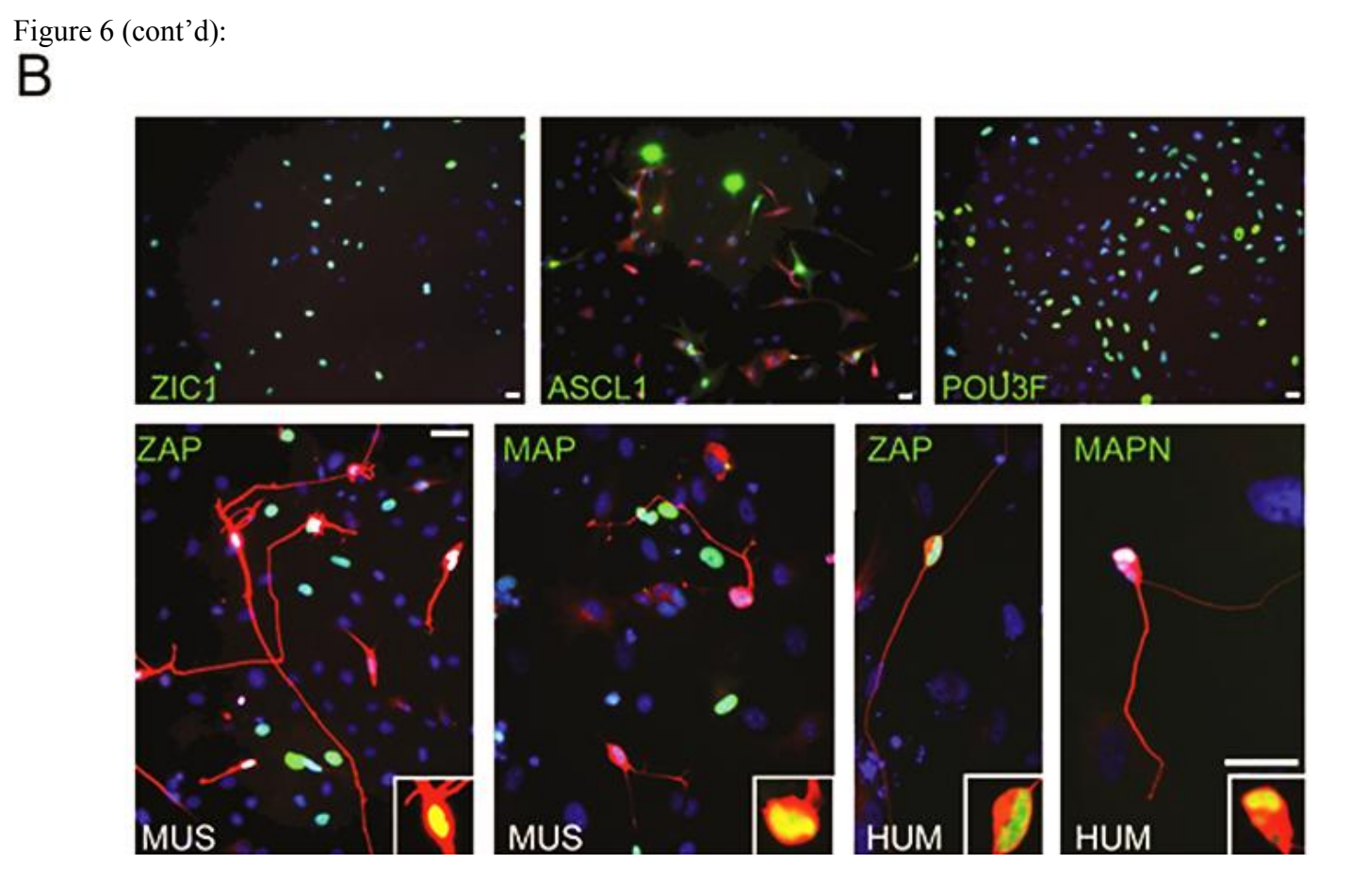
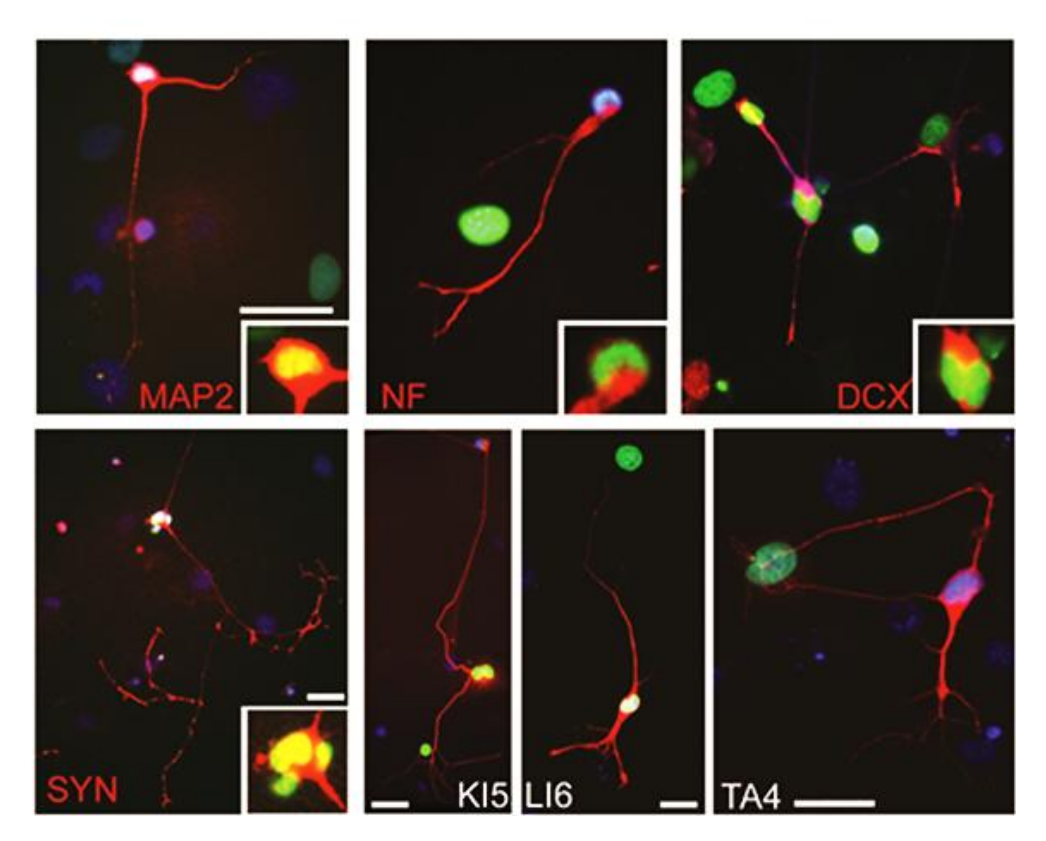


Figure 6 (cont'd):



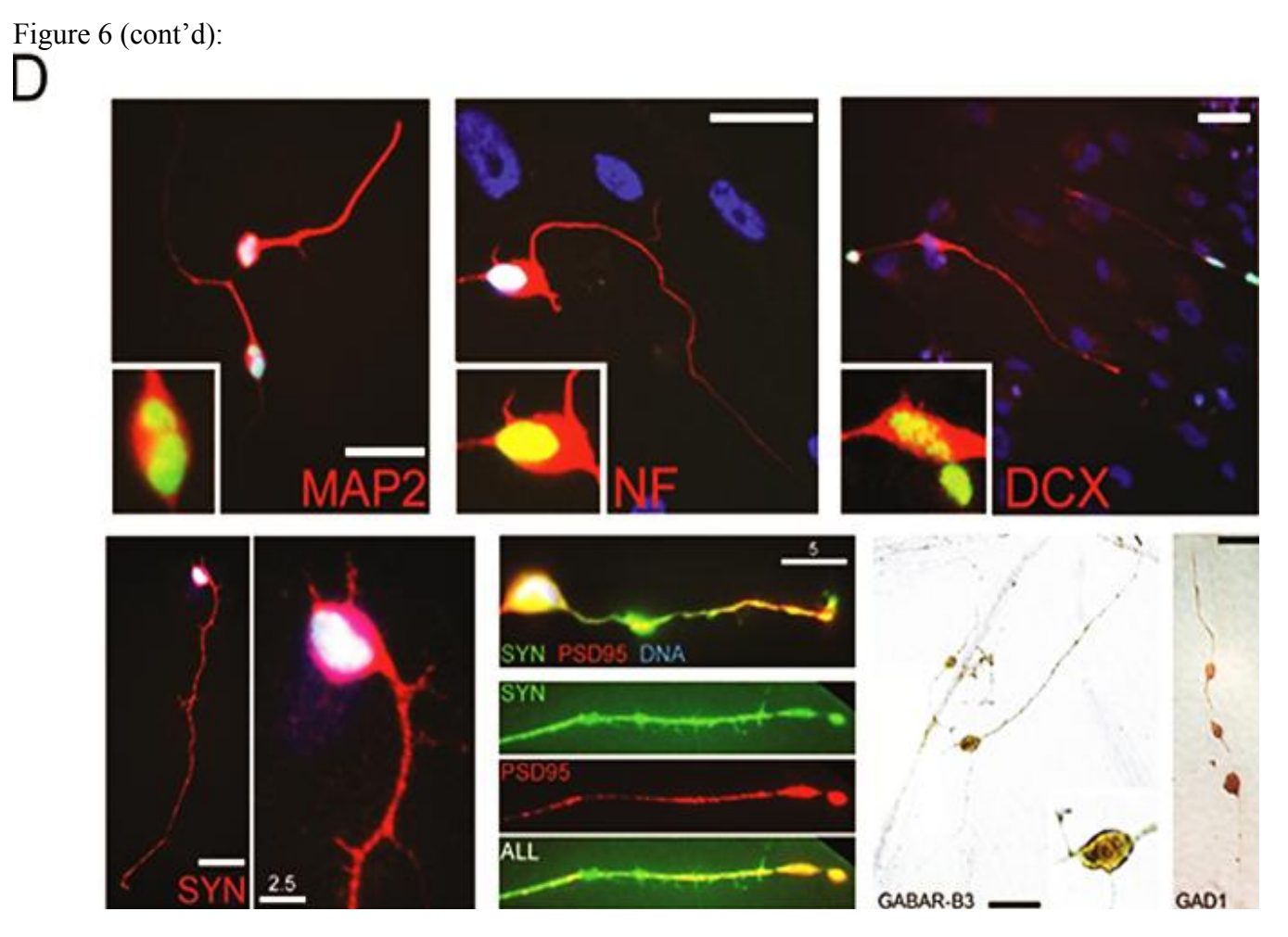


Figure 6 (cont'd): β -III-tubulin/TUJ1 in red (upper panels). Mouse (MEFs) or human fibroblasts (FET) infected with combinations of Zic1/ Ascl1/Pou3f2 (ZAP) or Myt1L/Ascl1/Pou3f2 (MAP) + NeuroD1 (MAPN) (lower panels). Green fluorescence indicates expression of reprogramming factor(s). Blue color is bis-benzimide nuclear staining of DNA. Insets have the blue channel removed and the green channel intensified to show YFP-factor expression in the nucleus of all iNCs. (C) Mouse iNCs produced from MEFs by day 10–15 post-infection immune positive for multiple neural markers Figure 6 (cont'd): (red), including MAP2, pan-neurofilament (NF), doublecortin (DCX), or synapsin I (SYN). iNCs produced from adult mouse fibroblast lines (as labeled) with typical iNC morphology immunostained for β -III-tubulin/TUJ1(red). (D) Human iNCs with typical morphology at day 24–30 post-infection and immunostained for multiple neuronal markers as in (C) in addition to PSD95, GABA receptor b 3 (GABARB3), and GAD1 (as labeled). GABAR-B3 and GAD1 iNCs were labeled using immunoperoxidase secondary antibody coupled with DAB staining. Scale bars are 10 mm unless otherwise labeled. (From Alicea et al. 2013 [54])

A

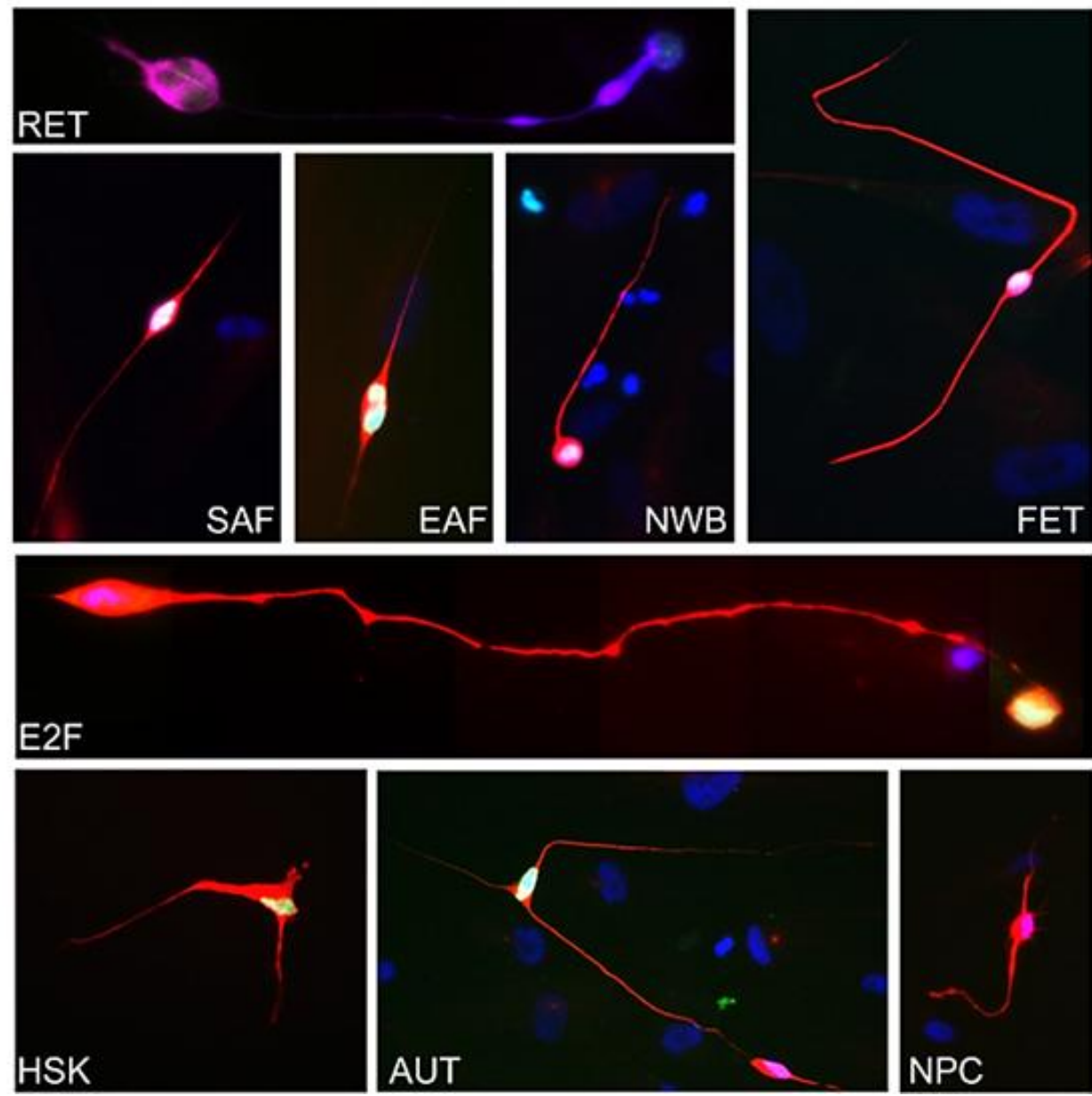
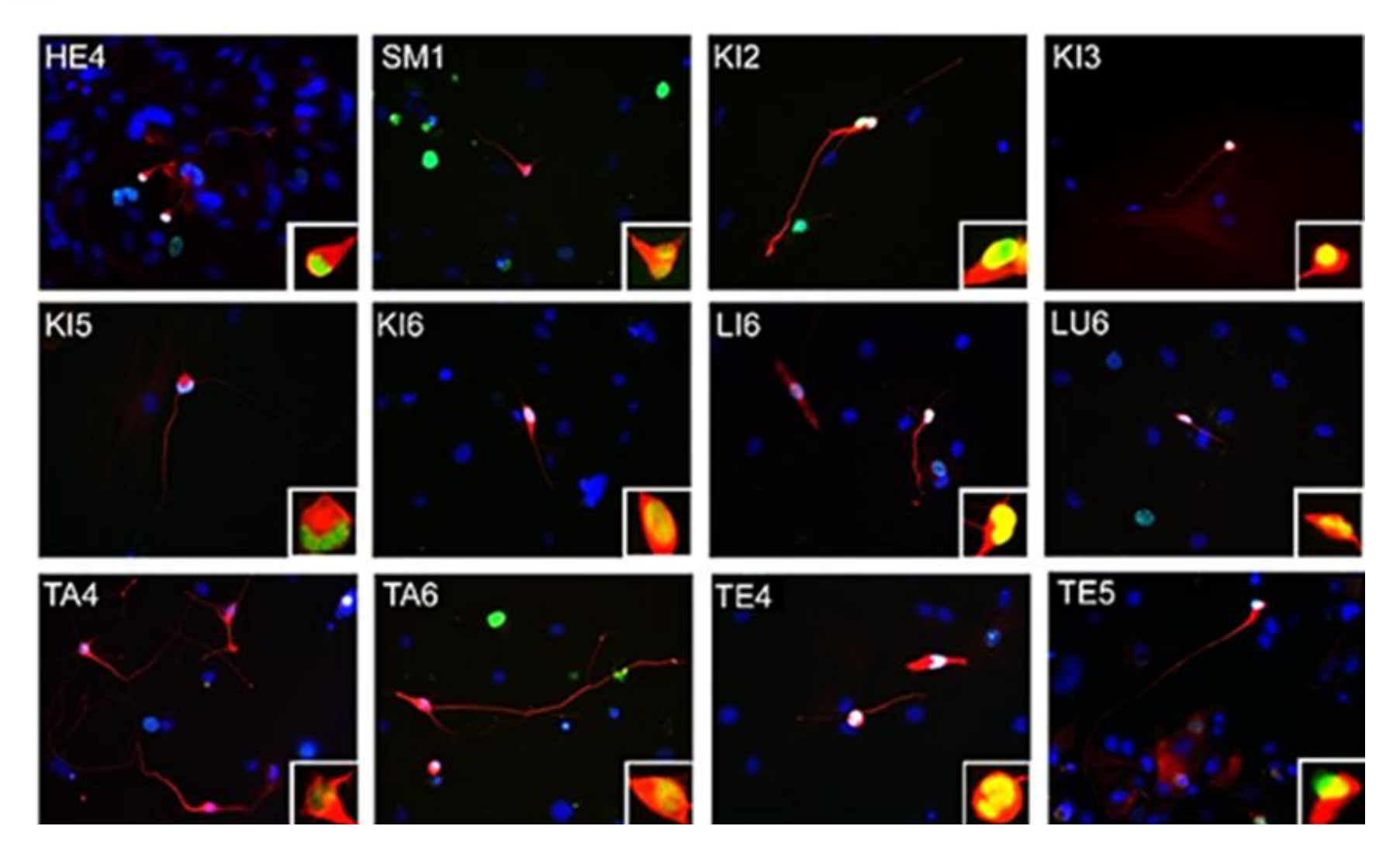


Figure 7: Representative images of β -III-tubulin/TUJ1 immuno-stained iNCs. (A) iNCs in human lines as labeled. Magnified insets have the blue channel removed and the green channel exaggerated to show factor expression in the iNC nucleus. All human lines produced iNCs, including AUT and HSK, that were not incorporated in the analysis. The iNCs shown in the E2F panel are a combination of multiple 1000X-magnification images. At the bottom right corner is a characteristic neuron produced from a human neural progenitor cell (NPC) differentiated in parallel with iNCs. (B) iNCs in mouse lines as labeled. Magnified insets have the blue channel removed and the green channel increased to show factor expression in the iNC nucleus.(From Alicea et al. 2013 [54])

Figure 7 (cont'd):





Not all cells had the capacity to take up the virus. Due to this limitation, we utilized another control for viral uptake. Each line was infected with a nuclearlocalized YFP virus at an MOI of approximately 0.5, and then counted to determine the number of cells with yellow fluorescent nuclei as a fraction of all cells at the time point of day 4 post-infection. By taking the previous calculation for reprogramming efficiency (red fluorescence value divided by the Hoechst 33342 fluorescence value), and dividing this by the YFP fluorescence value (indicative of cells that were able to uptake the virus at 4 days post-infection), the number of cells that would uptake the virus and change their phenotype into an iNC morphology could be compared with the number of cells with the ability to uptake the virus at all. As demonstrated in Figure 8 below, even when the variable of ability for a cell to uptake a virus is accounted for, a wide range of reprogramming efficiencies exists between different cell lines. It is important to note that each cell lines reprogramming regimen was repeated three times and those individual results were reproducible.

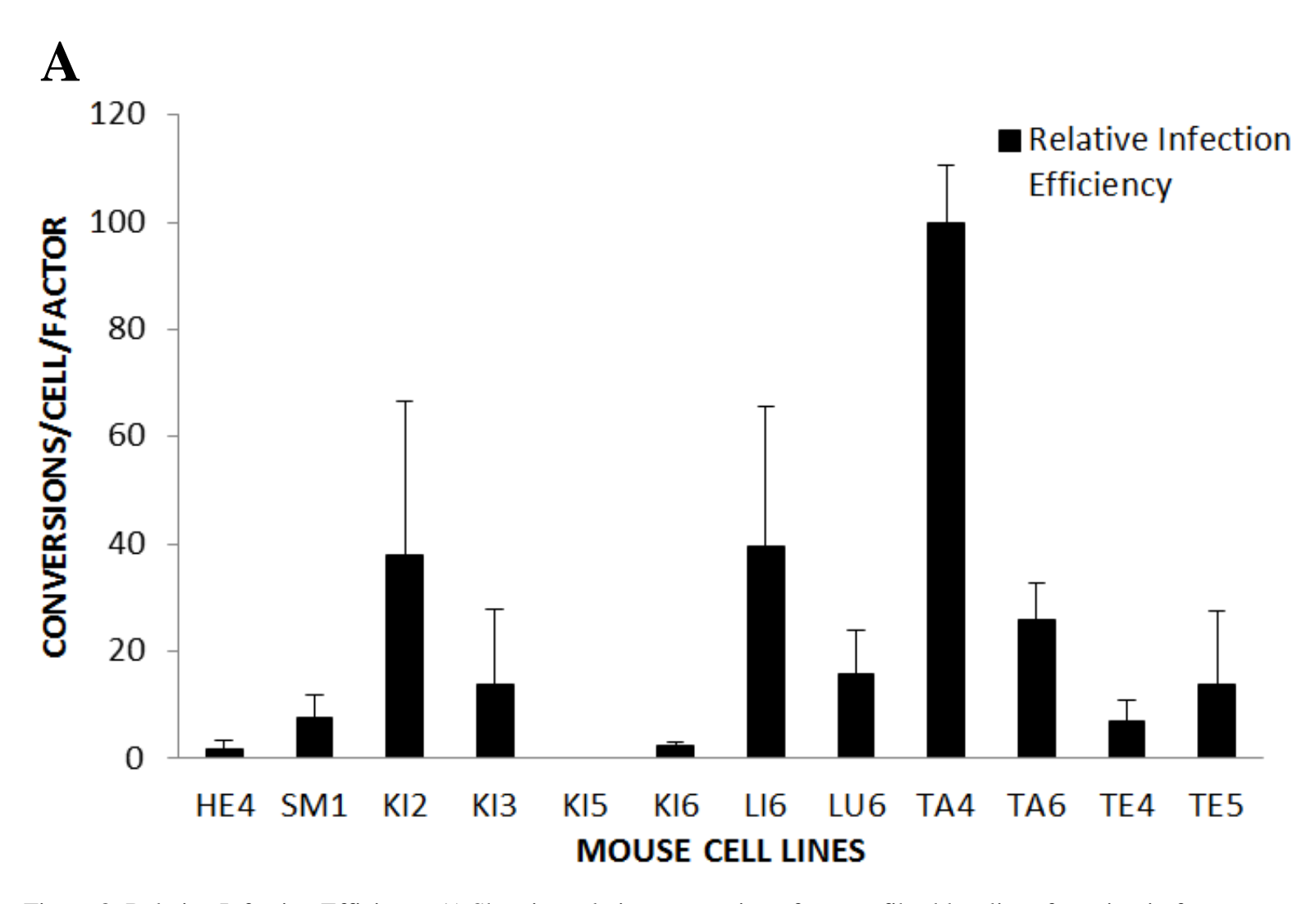
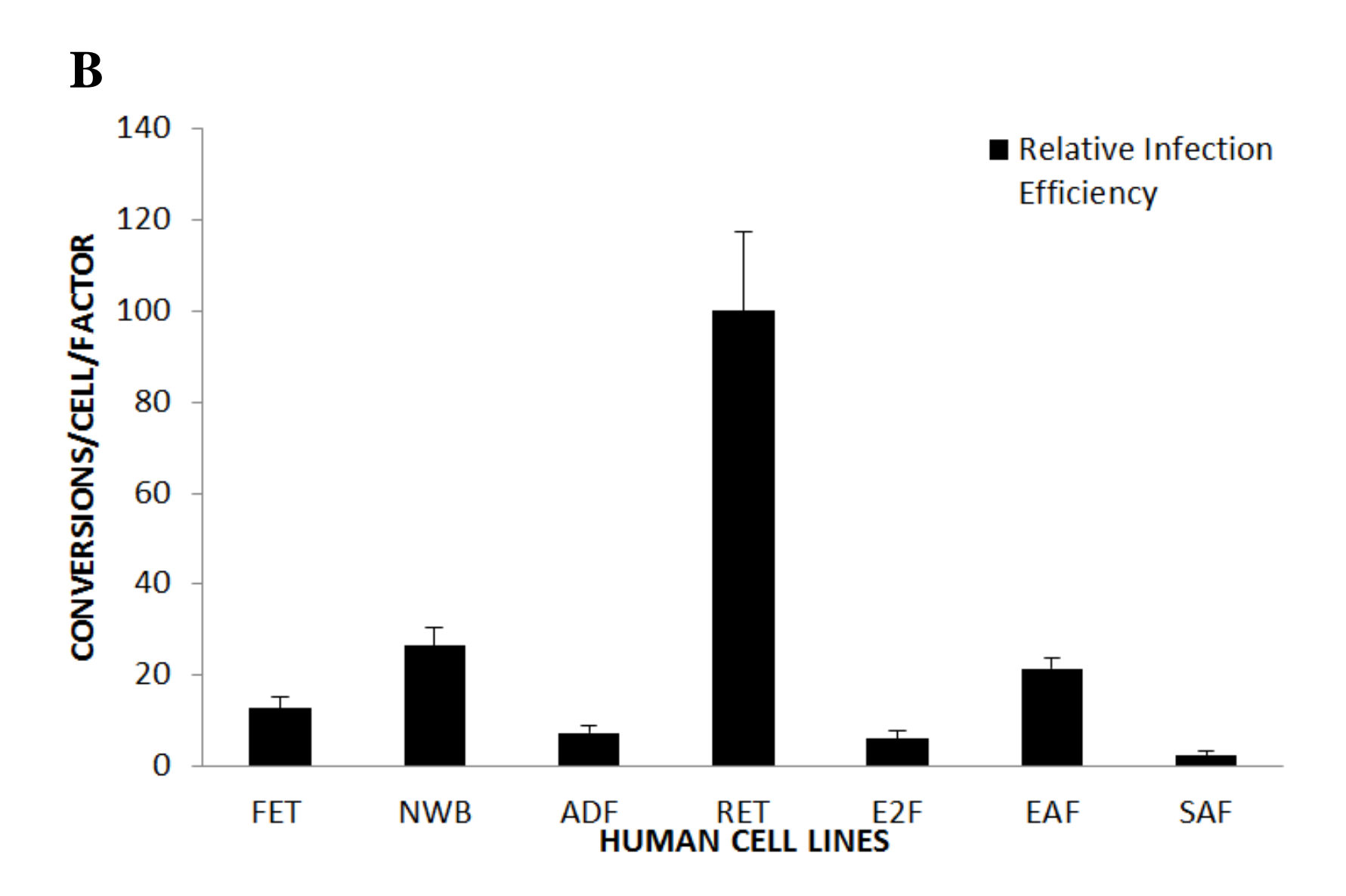


Figure 8: Relative Infection Efficiency A) Showing relative conversion of mouse fibroblast lines factoring in factor expression at day 4 post-infection. The highest efficiency of conversion within each group was set to a value of 100. Bars indicate standard error of the mean (SEM). B) As in A, for the human fibroblast lines.

Figure 8 (cont'd):



CONCLUSIONS

Here we strived to address several fundamental questions regarding the existence of variation in the cellular conversion efficiency between disease subtypes, genetic backgrounds, and tissue origin via conversion of fibroblasts to iNCs. We were able to demonstrate that the direct reprogramming capacity of independent primary fibroblast cell lines was reproducible within a single line from experiment to experiment, however the capacity varied dramatically from line to line. Through analysis of multiple cell lines derived from the same mouse, drastic differences of conversion efficiency displayed between different tissue types and even within the same tissue of origin were discovered. A certain genetic background does not necessarily play a large role in conversion efficiency into iNCs. The two human cell lines isolated from patients with neurological disease (RET and SAF) displayed reprogramming efficiencies that were at opposite ends of the spectrum with regard to iNC conversion. However, until a much higher number of lines from multiple patients are compared directly, these differences are likely to arise by chance.

Varying conversion rates are prompting the scientific community question what truly defines a "stem cell" and what is a truly "differentiated cell". Further questions continue to be raised regarding how some of these lines do not show any positivity for stem cell characteristics, however the fibroblasts included may have the intrinsic ability to go down a different path and therefore may not be "forced" down a program but altering the displayed program to another intrinsic program. Comi et al. reports that ASCL1 expression pushes human astrocytes down a neural phenotypic path *in vitro* and *in vivo* with methylation analysis indicative of epigenetic modification being the cause [50]. Via DNA Methylation Find-Peaks analysis they found regions of enriched methylation. It is possible that future definitions of cell types will rely on epigenetic

marks instead of phenotypic characteristics of the cells. The terminology is in question and further advances must be made to determine how fibroblasts are similar and variable to iNCs. Is there really homogeneity of fibroblast lines at an individual fibroblast cell level? With different microenvironments, this is unlikely.

Here we analyzed iNCs as having processes that are 3 cell bodies in length based on the findings of Vierbuchen described above [15]. Through application of this specification, we are excluding cells with shorter processes that may have required more time to mature. We are also excluding the possibility that those shorter processes may have equal or greater functionality in comparison with those processes of conventional length. Further longitudinal studies must be conducted to truly analyze the ability of fibroblasts to convert and function as iNCs.

Applied here was a viral delivery method. As a result, clinical application becomes less of a reality in the future because these vectors were once active viruses that were used to infect an animal or bacteria with a harmful disease. This is not a large risk to the patients; however there are alternative ways to introduce transcription factors into target cells that may be worth exploration. Adler et al. reports the use of plasmids encoding neuronal transcription factors to primary mouse embryonic fibroblasts with bioreducible linear poly(amino amine), stating there is low toxicity and high transfection efficiency. Hence repeated doses of these transcription factors can be delivered. However, their conversion rate measured was only 7.6% of cells were Tuj1 positive and only a subset of these was MAP2 positive [50]. An alternate delivery method of transcription factors may be required for translational use of conversion. Nevertheless, other options currently like the one reported by Adler et al. are average at best, if not subpar in comparison with the current viral delivery method.

There have been published reports on the ability to generate multipotent neural stem cells from mouse and human fibroblasts [51, 52]. Thier et al. reported conversion to multipotent neural stem cells with the ability to undergo over 50 passages while maintaining their marker expression profile and differentiation capacity. They discovered that the neural stem cells appeared to be activated by an intrinsic neural stem cell transcriptional program without dependence on sustained transgene expression [51]. Ring et al. reported using only the single transcription factor Sox2 to generate functional neurons that can integrate, survive, and be multipotent *in vivo* without tumor formation [52]. The capability to generate a neural stem cell has advantages related with the ability to produce multiple cell types including manifold types of mature neurons, astrocytes, and oligodendrocytes. Furthermore, the capacity to self-renew becomes a possibility. However the generation of the neural stem cells is at a very low efficiency and has not been thoroughly tested on multiple cell lines from non-embryonic fibroblast sources. Thus, exhibiting the same difficulties direct conversion of fibroblasts into neurons has shown.

The media portrays cellular reprogramming as a process that will be clinically available in the near future. In reality however there are basic mechanisms that are not understood, and must be addressed regarding conversion efficiency. Great strides have been made in an attempt to make this therapy viable and readily available to the masses. Torper et al. reported the successful direct neural conversion of transplanted human and endogenous mouse cells *in vivo* in a rodent brain, thereby substantiating for the first time that neural conversion is possible *in vivo* [53]. Despite the findings by Torper et al., many hurdles still exist and must be addressed. In reality, we are at a standstill because we have not yet identified the precise differences between different fibroblasts that are responsible for variation in the efficiency of cellular reprogramming

into a different phenotype. Until this is addressed and understood, cellular reprogramming is not yet ready for clinical deployment to the masses as a treatment option.

Until populations of input cells such as fibroblasts are better characterized as both individual cells and cell populations, there will likely continue to be issues with regard to the reliability of reprogramming. Clinical application is pending answers to these questions and labor intensive work has to be completed in order to achieve medical application.

REFERENCES

REFERENCES

- 1. Brock A, Goh HT, Yang B, Lu Y, Li H, Loh YH. (2012). Cellular reprogramming: a new technology frontier in pharmaceutical research. Pharm Res. 1:35-52.
- 2. Baptiste, D.C., and Fehlings, M.G. (2007). Update on the treatment of spinal cord injury. Prog. Brain Res. 161, 217–233.
- 3.Barnabe-Heider, Fanieand Frisen, Jonas (2008). Stem Cells for Spinal Cord Repair. Cell Stem Cell. 3, 16-24.
- 4. N. Rodriguez-Osorio, R. Urrego, J.B. Cibelli, K. Eilertsen, E. Memili. (2012). Reprogramming mammalian somatic cells. Theriogenology. 78, 1869-1886.
- 5. Holliday R. The inheritance of epigenetic defects. Science 1987;238:163–70.
- 6. Boron, W. F., Boulpaep, E.L. (2005). Medical Physiology, Updated Edition. Philedelphia, PA: Elsevier Saunders.
- 7. Robert L. Davis, H. W., and Andrew B. Lassar (1987). Expression of a Single Transfected cDNA Converts Fibroblasts to Myoblasts. Cell 51: 987-1000.
- 8. Kunhua Song, Y.-J. N., Xiang Luo, Xiaoxia Qi, Wei Tan, Guo N. Huang, AshaAcharya, Christopher L. Smith, Michelle D. Tallquist, Eric G. Neilson, Joseph A. Hill, Rhonda Bassel-Duby& Eric N. Olson (2012). Heart repair by reprogramming non-myocytes with cardiac transcription factors. Nature 485: 599-604.
- 9. Ernesto Lujan, S. C., HenrikAhlenius, Thomas C. Südhof, and Marius Wernig (2011). Direct conversion of mouse fibroblasts to self-renewing, tripotent neural precursor cells. PNAS 109(7): 2527-2532.
- 10. Nakamura M, Okano H. (2013). Cell transplantation therapies for spinal cord injury focusing on induced pluripotent stem cells. Cell Res. 1:70-80.
- 11. Steinemann D, Gohring G, Schlegelberger B. (2013). Genetic instability of modified stem cells a first step towards malignant transformation? Am J Stem Cells. 2(1): 39-51.
- 12.Drews K, Jozefczuk J, Prigione A, Adjaye J. (2012). Human induced pluripotent stem cells—from mechanisms to clinical applications. J Mol Med (Berl). 90 (7): 735-745.
- 13. Davis RL, H Weintraub and AB Lassar. (1987). Expression of a single transfected cDNA converts fibroblasts to myoblasts. Cell 51:987–1000.

- 14. Takahashi K and S Yamanaka. (2006). Induction of pluripotent stem cells from mouse embryonic and adult fibroblast cultures by defined factors. Cell 126:663–676.
- 15. Vierbuchen T, AOstermeier, ZP Pang, Y Kokubu, TC Sudhof and M Wernig. (2010). Direct conversion of fibroblasts to functional neurons by defined factors. Nature 463:1035–1041.
- 16. Ieda M, JD Fu, P Delgado-Olguin, V Vedantham, Y Hayashi, BG Bruneau and D Srivastava. (2010). Direct reprogramming of fibroblasts into functional cardiomyocytes by defined factors. Cell 142:375–386.
- 17. Huang P, Z He, S Ji, H Sun, D Xiang, C Liu, Y Hu, X Wang and L Hui. (2011). Induction of functional hepatocyte-like cells from mouse fibroblasts by defined factors. Nature 475:386–389.
- 18.Lattanzi L, G Salvatori, M Coletta, C Sonnino, MG Cusella De Angelis, L Gioglio, CE Murry, R Kelly, et al. (1998). High efficiency myogenic conversion of human fibroblasts by adenoviral vector-mediated MyoD gene transfer. An alternative strategy for ex vivo gene therapy of primary myopathies. J Clin Invest 101:2119–2128.
- 19. Yoshida Y and S Yamanaka. (2012). Labor pains of new technology: direct cardiac reprogramming. Circ Res 111:3–4.
- 20. Song K, YJ Nam, X Luo, X Qi, W Tan, GN Huang, A Acharya, CL Smith, MD Tallquist, et al. (2012). Heart repair by reprogramming non-myocytes with cardiac transcription factors. Nature 485:599–604.
- 21. Chen JX, M Krane, MA Deutsch, L Wang, M Rav-Acha, S Gregoire, MC Engels, K Rajarajan, R Karra, et al. (2012). Inefficient reprogramming of fibroblasts into cardiomyocytes using Gata4, Mef2c, and Tbx5. Circ Res 111:50–55.
- 22. Satelli A, L. S. (2011). Vimentin in cancer and its potential as a molecular target for cancer therapy. Cell Mol Life Sci. 18: 3033-3046.
- 23. Mettouchi A. (2012). The role of extracellular matrix in vascular branching morphogenesis. Cell AdhMigr. 6:528-534.
- 24. Bahi-Buisson N. (2013). Genetically determined encephalopathy: Rett syndrome. HandbClin Neurol. 111:281-286.
- 25. Maria Chahrour and Huda Y. Zogbi (2007). The Story of Rett Syndrome: From Clinic to Neurobiology. Neuron. 56: 422-437.
- 26. Hagberg, B. (2005). Rett syndrome: long-term clinical follow-up experiences over four decades. J. Child Neurol. 20, 722–727.

- 27. Roze, E., Cochen, V., Sangla, S., Bienvenu, T., Roubergue, A., Leu-Semenescu, S., and Vidaihet, M. (2007). Rett syndrome: An overlooked diagnosis in women with stereotypic hand movements, psychomotor retardation, Parkinsonism, and dystonia? Mov.Disord. 22, 387–389.
- 28. Armstrong, D.D. (2005). Neuropathology of Rett syndrome. J. Child Neurol. 20, 747–753.
- 29. Jellinger, K., Armstrong, D., Zoghbi, H.Y., and Percy, A.K. (1988). Neuropathology of Rett syndrome. Acta Neuropathol. (Berl.) 76, 142–158.
- 30. Reiss, A.L., Faruque, F., Naidu, S., Abrams, M., Beaty, T., Bryan, R.N., and Moser, H. (1993). Neuroanatomy of Rett syndrome: a volumetric imaging study. Ann. Neurol. 34, 227–234.
- 31. Mattai AK, Hill JL, Lenroot RK. (2010). Treatment of early-onset schizophrenia. CurrOpin Psychiatry. 23(4): 304-310.
- 32. Murphy BP. (2012). Beyond the first episode: candidate factors for a risk prediction model of schizophrenia. Int Rev Psychiatry. 22(2):202-223.
- 33. Vita A, De Peri L, Deste G, Sacchetti E. (2012). Progressive loss of cortical gray matter in schizophrenia: a meta-analysis and meta-regression of longitudinal MRI studies. Transl. Psychiatry. 2:e190.
- 34. Suhr ST, EA Chang, RM Rodriguez, K Wang, PJ Ross, Z Beyhan, S Murthy and JB Cibelli.(2009). Telomere dynamics in human cells reprogrammed to pluripotency.PLoS One 4:e8124.
- 35. Hamill OP, A Marty, E Neher, B Sakmann and FJ Sigworth. (1981). Improved patch-clamp techniques for high-resolution current recording from cells and cell-free membrane patches. Pflugers Arch 391:85–100.
- 36. Chang EA, Z Beyhan, MS Yoo, K Siripattarapravat, T Ko, KJ Lookingland, BV Madhukar and JB Cibelli. (2009). Increased cellular turnover in response to fluoxetine in neuronal precursors derived from human embryonic stem cells. Int J DevBiol 54:707–715.
- 37. Day K, G Shefer, A Shearer and Z Yablonka-Reuveni. (2010). The depletion of skeletal muscle satellite cells with age is concomitant with reduced capacity of single progenitors to produce reserve progeny. DevBiol 340:330–343.
- 38. Day K, G Shefer, JB Richardson, G Enikolopov and Z Yablonka-Reuveni. (2007). Nestin-GFP reporter expression defines the quiescent state of skeletal muscle satellite cells. DevBiol 304:246–259.

- 39. Ellis P, BM Fagan, ST Magness, S Hutton, O Taranova, S Hayashi, A McMahon, M Rao and L Pevny. (2004). SOX2, a persistent marker for multipotential neural stem cells derived from embryonic stem cells, the embryo or the adult. DevNeurosci 26:148–165.
- 40. D'Amour KA and FH Gage. (2003). Genetic and functional differences between multipotent neural and pluripotent embryonic stem cells. ProcNatlAcadSci U S A 100 Suppl 1:11866–11872.
- 41. Vogel W, F Grunebach, CA Messam, L Kanz, W Brugger and HJ Buhring. (2003). Heterogeneity among human bone marrow-derived mesenchymal stem cells and neural progenitor cells. Haematologica 88:126–133.
- 42. Avilion AA, SK Nicolis, LH Pevny, L Perez, N Vivian and R Lovell-Badge. (2003). Multipotent cell lineages in early mouse development depend on SOX2 function. Genes Dev 17:126–140.
- 43. Zimmerman L, B Parr, U Lendahl, M Cunningham, R McKay, B Gavin, J Mann, G Vassileva and A McMahon. (1994). Independent regulatory elements in the nestin gene direct transgene expression to neural stem cells or muscle precursors. Neuron 12:11–24.
- 44. Pfisterer U, A Kirkeby, O Torper, J Wood, J Nelander, ADufour, A Bjorklund, O Lindvall, J Jakobsson and M Parmar. (2011). Direct conversion of human fibroblasts to dopaminergic neurons. ProcNatlAcadSci U S A 108: 10343–10348.
- 45. Pang ZP, N Yang, T Vierbuchen, A Ostermeier, DR Fuentes, TQ Yang, A Citri, V Sebastiano, S Marro, TC Sudhof and M Wernig. (2011). Induction of human neuronal cells by defined transcription factors. Nature 476:220–223.
- 46. Caiazzo M, MT Dell'anno, E Dvoretskova, D Lazarevic, S Taverna, D Leo, TD Sotnikova, A Menegon, P Roncaglia, et al. (2011). Direct generation of functional dopaminergic neurons from mouse and human fibroblasts. Nature 476: 224–227.
- 47. Ambasudhan R, M Talantova, R Coleman, X Yuan, S Zhu, SA Lipton and S Ding. (2011). Direct reprogramming of adult human fibroblasts to functional neurons under defined conditions. Cell Stem Cell 9:113–118.
- 48. Chang HY, JT Chi, S Dudoit, C Bondre, M van de Rijn, D Botstein and PO Brown. (2002). Diversity, topographic differentiation, and positional memory in human fibroblasts.ProcNatlAcadSci U S A 99:12877–12882.
- 49. Corti S, Nizzardo M, Simone C, Falcone M, Donadoni C, Salani S, Rizzo F, Nardini M, Riboldi G, Magri F, Zanetta C, Faravelli I, Bresolin N, Comi GP. (2012). Direct reprogramming of human astrocytes into neural stem cells and neurons. Exp Cell Res. 318(13):1528-1541.

- 50. Adler AF, Grigsby CL, Kulangara K, Wang H, Yasuda R, Leong KW. (2012). Nonviral direct conversion of primary mouse embryonic fibroblasts to neuronal cells. MolTher Nucleic Acids.1:e32.
- 51. Thier M, Wörsdörfer P, Lakes YB, Gorris R, Herms S, Opitz T, Seiferling D, Quandel T, Hoffmann P, Nöthen MM, Brüstle O, Edenhofer F. (2012). Direct conversion of fibroblasts into stably expandable neural stem cells. Cell Stem Cell. 10(4):473-479.
- 52. Ring KL, Tong LM, Balestra ME, Javier R, Andrews-Zwilling Y, Li G, Walker D, Zhang WR, Kreitzer AC, Huang Y. (2012). Direct reprogramming of mouse and human fibroblasts into multipotent neural stem cells with a single factor. Cell Stem Cell. 11(1):100-109.
- 53. Torper O, Pfisterer U, Wolf DA, Pereira M, Lau S, Jakobsson J, Björklund A, Grealish S, Parmar M. (2013). Generation of induced neurons via direct conversion in vivo.ProcNatlAcadSci U S A.110(17):7038-7043.
- 54. Alicea B, Murthy S, Keaton SA, Cobbett P, Cibelli JB, Suhr ST. (2013). Defining the Diversity of Phenotypic Respecification Using Multiple Cell Lines and Reprogramming Regimens. Stem Cells Dev. [Epub ahead of print]